THESIS

HIGH PRESSURE VAPOR-LIQUID EQUILIBRIUM MEASUREMENTS OF METHANE AND WATER MIXTURES USING NUCLEAR MAGNETIC RESONANCE SPECTROSCOPY

Submitted by

Michael Sartini

Department of Mechanical Engineering

In partial fulfillment of the requirements

For the Degree of Master of Science

Colorado State University

Fort Collins, Colorado

Spring 2021

Master's Committee:

Advisor: Dr. Bret C. Windom

Dr. Jason Widegren
Dr. Nancy Levinger

ABSTRACT

HIGH PRESSURE VAPOR-LIQUID EQUILIBRIUM MEASUREMENTS OF METHANE AND WATER MIXTURES USING NUCLEAR MAGNETIC RESONANCE SPECTROSCOPY

Gas composition, which can vary from location to location in natural gas pipelines, constrains the allowable operating conditions and compressor package design. Compressor systems are designed such that they provide the optimal balance between efficiency and gas throughput with safety margins to maintain component lifetime. The presence of liquid in the compressor can lead to excessive wear of intake and discharge valves and impact performance. To prevent ingestion of liquid slugs, operating conditions and separation equipment must be selected appropriately using mixture dew point calculations from commercially available mixture property prediction software such as NIST-REFPROP. NIST-REFPROP is highly reliant on mixture Vapor-liquid Equilibrium (VLE) data to predict phases. Thus, there is a need for low uncertainty VLE data for gas mixtures at pressures (1 - 10 MPa) and temperatures (<0 – 100 °C) experienced within natural gas infrastructure, especially for mixtures containing H_2O, which would lead to more accurate dew point calculations and allow designers to maximize system performance without compromising component wear and tear. For a mixture comprised completely of hydrocarbon species, VLE calculations at high pressures are accurate as the interaction parameters between the constituents are close to unity and there is typically a wealth of low-uncertainty data available. However, when H_2O is present in natural gas significant intermolecular interactions cause the mixture VLE to deviate from ideality. In order to accurately model the VLE of these mixtures, the

energy associated with these interactions must be known and accounted for in the calculations. As such, high quality experimental VLE data are needed to improve and validate the thermodynamic models. Nuclear magnetic resonance (NMR) spectroscopy allows for high-quality data collection for water containing samples. This thesis provides the groundwork for using NMR spectroscopy to conduct low-uncertainty VLE measurements of water-hydrocarbon mixtures. Two NMR spectrometers were investigated, and methods were developed to accurately characterize the temperature, pressure, vapor phase and liquid phase molar composition of methane-water systems at equilibrium, the five conditions required for VLE measurement. Preliminary results for low pressure (0-2.06MPa) samples of methane and water showed that the liquid phase methane compositional data taken utilizing NMR spectroscopy significantly deviated from the NIST-REFPROP model, revealing the lack of low uncertainty VLE data required to determine the needed interaction parameters for methane and water systems. Future work should target the collection of the high-fidelity methane-water VLE data, and NMR spectroscopy has the potential to perform this task.

ACKNOWLEDGEMENTS

I would first like to thank my advisor Dr. Bret Windom for his excellent support and guidance throughout the entirety of the project. Whenever there was a project hiccup, he always knew how to guide me in the right direction to continue.

I would also like to thank the Dr. Jason Widegren, Dr. Christopher Suiter, and Dr. Mark McLinden for their project guidance and NMR expertise to help formulate proper experimental procedures for the entire project. A special thanks to Dr. Christopher Suiter for all NMR experimental data collection assistance!

Finally, I would like to thank my parents for their unconditional support and encouragement throughout my educational career. I would not be here where I am today without them.

TABLE OF CONTENTS

LIST OF TABLES

LIST OF FIGURES

1. INTRODUCTION

Natural gas is one of the most used and versatile resources in the United States. It is made up of several different organic compounds, with the large majority being methane. Common applications of this resource are in space heating, water heating, cooking, and electricity[1]. This residential and commercial versatility causes a large demand across the country. In recent years this demand for natural gas has increased up to roughly one third of the total 106 exajoules (EJ) of energy consumed in the United States[2]. With this increased demand gas transportation methods are required scale up accordingly. The current gas transportation method is through a nationwide network of pipelines with compressor stations about every 50 miles (Figure 1).

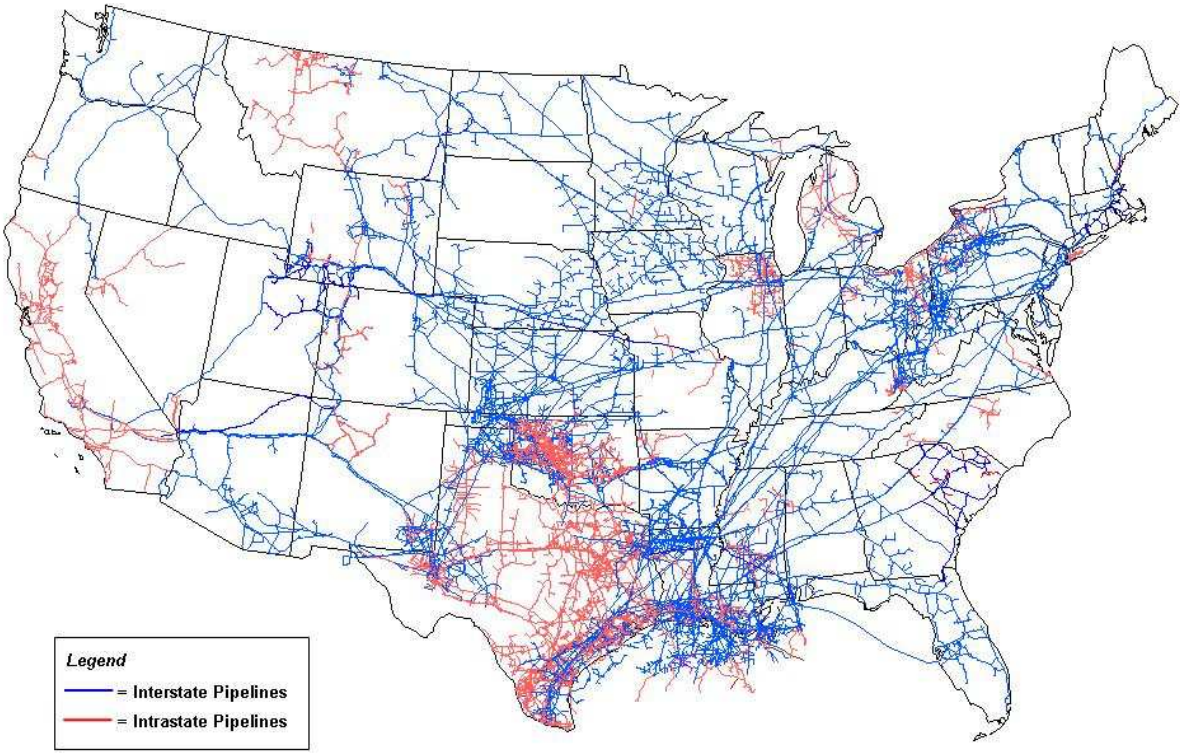

Figure 1: The United States natural gas pipeline network in the lower 48 states. More than 305,000 miles of interstate and intrastate pipelines and 1,400 compressor stations in order to maintain pressure[3].

The purpose of these compressor stations is to compensate for the frictional pressure loss that the gas experiences through these long sections of pipes. Due to the large geographic scale of this operation, about 3% of the total natural gas used in the United States, roughly 1 exajoule, is used for gas transportation[1]. With this large energy transportation cost even the smallest efficiency improvement in gas delivery will lead to significant savings.

The transportation of natural gas is largely decreased when any presence of liquid is within the system. This is due to the decreased mobility of natural gas when condensation occurs. There are methods to remove this condensate but they involve large equipment to separate these two phases, ultimately requiring maintenance and operational costs. This liquid condensate not only affects the gas throughput on a normal operational day but could also freeze when conditions permit. Texas in the middle of February 2021 experienced natural gas outages across the state due to frigid temperatures. It was later determined that the cause of these outages were due to both separation equipment and general equipment freezing[4]. These freezing conditions caused millions of Americans not to have heat or electricity for weeks. With better separation process designs these outages would have been less severe and taken less time to bring back into operating conditions.

This gas composition constrains the allowable operating conditions and compressor package designs. To prevent this development and ingestion of liquid slugs, operating conditions and separation equipment must be selected appropriately using mixture dew point calculations from commercially available equation of state solving software such as NIST-REFPROP or Aspen Hysys.

1.2. CONDENSATION

The condensation that can develop in natural gas pipelines can be visualized by constructing phase diagrams to help demonstrate this thermodynamic behavior. Two key characteristics of phase diagrams are their phases and transitional points. These key characteristics of a phase diagram are known as the critical point, dew point curve, bubble point curve, cricondentherm, and cricondenbar (Figure 2).

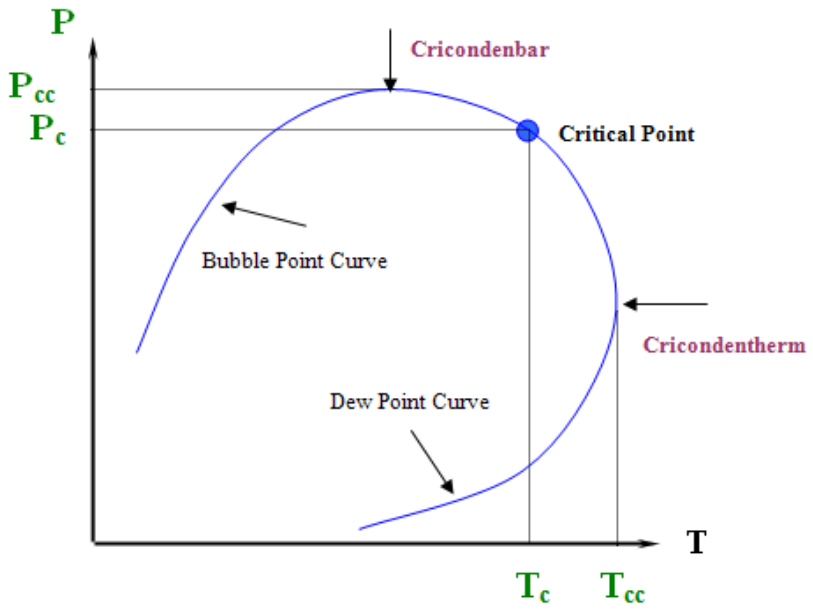

Figure 2: Phase diagram highlighting the major characteristics[5]. P_{cc} is corresponding to the cricondenbar. T_{cc} is corresponding to the cricondentherm. And T_c and P_c are corresponding to the critical point.

This diagram describes three possible states that the mixture could be in: liquid, vapor, or two-phase. Inside the curve is known as the two-phase region, it is bounded by the cricondentherm and cricondenbar. These are the maximum temperature and pressure where two phases are able exist, respectively. The curve that is to the left of the critical point is known as the bubble point curve; this separates the two-phase region from the only liquid region. Likewise, right of the critical point is the dew point curve where it separates the two-phase region from the vapor region. Keeping this

phase diagram in mind, in natural gas pipelines pressures tend to naturally decrease the further from the compressor. This characteristic is due to the friction that the gas experiences in the transportation process. On the phase diagram this would be represented from starting from the top of the y-axis and heading downward. Contrary to expectations, some gas mixture will condense to a liquid as the pressure decreases until maximum dropout occurs. This phenomenon is called retrograde condensation[5].

To help illustrate under what conditions this condensation occurs, we must look at the phase diagram of a general hydrocarbon mixture (Figure 3)

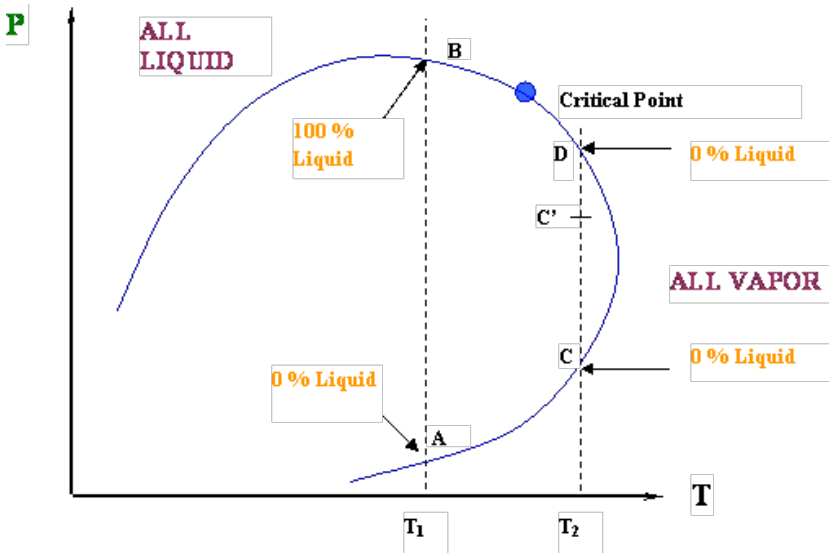

Figure 3: General phase diagram highlighting two different isothermal compressions. At T_2 retrograde condensation occurs between points C and D[5].

Figure 3 highlights two different isothermal conditions that a mixture could experience. Option B-A is an example where due to expansion the mixture is going from 100% liquid to 0% liquid. In between the two extremes, the two-phase region contains some mixture of both liquid and vapor phases. The second option, D-C, where temperatures are in between the critical point and cricondentherm, the mixture is bounded by two points of 0% liquid. Knowing the characteristics of a phase diagram, inside the bounded area, there must exist a two-phase mixture. This means

that between both 0% liquid boundaries, there must exist conditions that produce some fraction of liquid phase. This characteristic of the phase diagram demonstrates this possibility of condensation occurring while pressure decreases.

Within these natural gas pipelines, gas throughput is one of the key parameters that is optimized. Natural gas mobility is increased significantly when still in a vapor phase. The production of liquid phase, through liquid drop-out, would decrease the mobility of the gas ultimately lowering the efficiency of the system. To help avoid this liquid phase production, designers utilize equation of state software in order to predict at what conditions liquid drop-out will occur. By knowing the exact conditions that will lead to liquid drop-out, operators are able to keep pressures throughout the system above that critical pressure. This demonstrates the significance of accurately knowing the characteristics of the hydrocarbon mixtures.

1.3. LITERATURE REVIEW

Liquid drop-out in natural gas pipelines is primarily due to retrograde condensation (see Section 1.2.). This phenomenon is bounded by the shape of the dew point curve for a specific mixture. Current studies directly measuring dew point conditions ultimately reveal the absence of repeatable experimental results and equation of state solutions. South West Research Institute (SWRI) looked into several natural gas mixtures using multiple different experimental methods[10]. One mixture in particular exhibited larger deviations than the others. This composition had 0.05% mole fraction of water incorporated into the mixture. With this mixture SWRI used a chilled mirror experiment and gas chromatograph (GC) to compare to the predicted dewpoint curve from an equation of state solution (Figure 4).

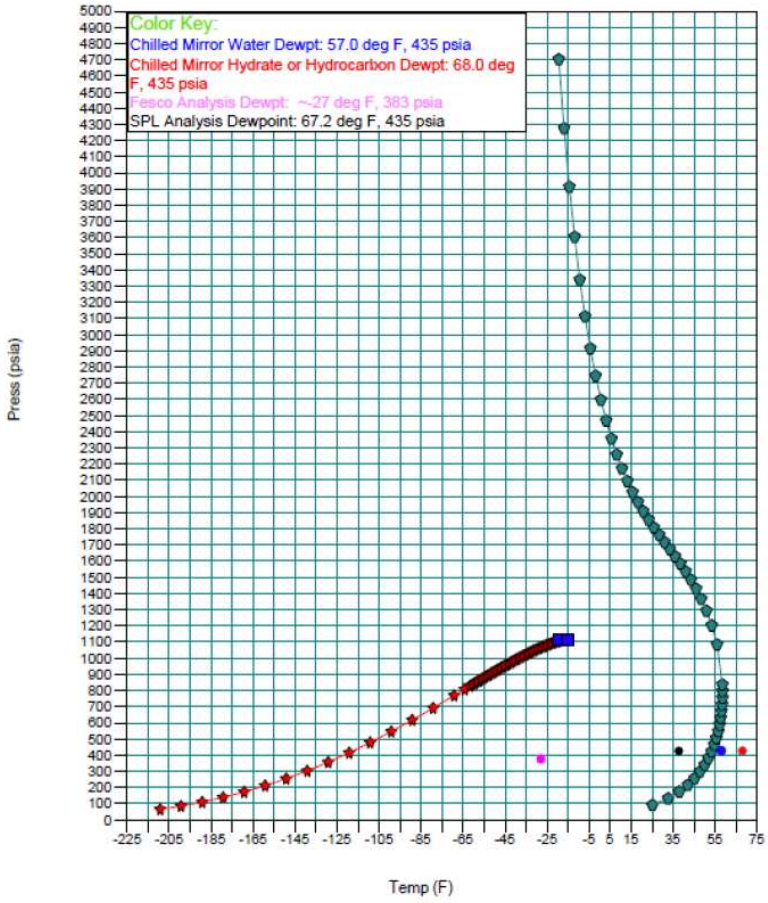

Figure 4: Comparison between experimental measurements of natural gas dew points from SWRI and the gas supplier's equation of state calculations. Four different colors representing the three methods utilized and one for the numerical model[10].

SWRI's reported dewpoint measurements at 400 psig ranged from 68°F to -27°F. This increased uncertainty was caused by several reported factors including component separation and mixture composition. Component separation stems from the diagnostic instrument's capabilities. The GC utilized in the study was unable to run samples with any amount of water. Therefore, samples were dehydrated and then compensated for in post processing. The mixture composition affected the accuracy of the standard experimental method. Even the simplest binary mixtures that contain water tend to have large discrepancies between datasets and ideal mixture models[8].

These equation of state (EOS) solving softwares are extremely important to accurately predict these non-ideal mixture interactions and conditions. The accurate predictions are dependent on data and ideal correlations to fit thermodynamic mixture models. Henry's Law and Raoult's Law are ideal correlations that are valid for a specific set of conditions in mixtures. Henry's Law states that the solubility of a gas (C) in a liquid is directly proportional to the partial pressure of the gas (P) multiplied by a constant (K_H) (Equation 1). It requires three conditions to be satisfied in order to predict solubility correctly: (1) the mixture is in equilibrium, (2) the pressure of the mixture is relatively low, and (3) there are no reactions between the constituents[13].

$$C = k_H * P \tag{1}$$

Raoult's law states that the vapor pressure of a mixture component above a solution ($P_{solution}$) is equal to the vapor pressure of the pure component ($P^o_{component}$) scaled by the mole fraction of the component ($x_{component}$) (Equation 2)[14].

$$P_{solution} = x_{component} * P^o_{component} \tag{4}$$

Similar to Henry's law, Raoult's Law requires for the mixture to be ideal. Both of these correlations are close to predicting the actual nonideal solution but only for a narrow set of conditions. Henry's Law is for low concentrations at low pressures and Raoult's Law is suited for high concentrations (near pure composition) (Figure 5).

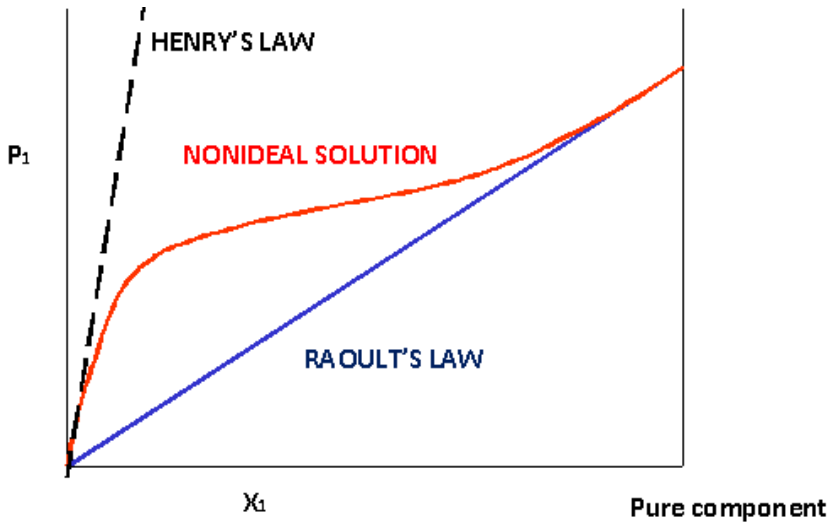

Figure 5: Non ideal behavior in vapor pressure (P_1) compared at low and high concentrations to Henry's Law and Raoult's Law, respectively[13,14].

Of the data utilized in the non-ideal mixture model regime, one of the most important data sets for fluid mixtures is vapor-liquid equilibrium (VLE) data. This VLE data is comprised of the temperature (T), pressure (P), and the relative composition (mole fraction) of both liquid (x) and vapor (y) phases at the sample's thermodynamic equilibrium (T, p, x, y) (Figure 6).

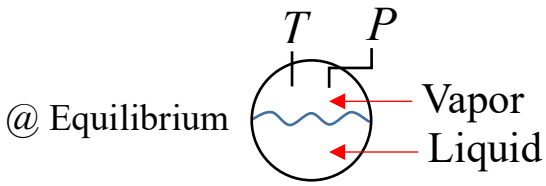

Figure 6: A visual representation of a closed system at equilibrium showing the four measurements that are needed to define the system (T, p, x, y).

A common characteristic of literature hydrocarbon VLE data is that there is either no data at relevant temperatures and pressures or there are too many data sets that ultimately reveal significant deviation and scatter. Methane + propane, an important natural gas mixture that has been extensively studied, illustrates this scatter in its VLE data compared to the GERG model of

Kunz and Wagner[6], which is a common equation of state for thermodynamic properties of natural gas mixtures. McLinden and Richter[7] have compared several studies to this GERG model (Figure 7) ultimately revealing this scatter of data points.

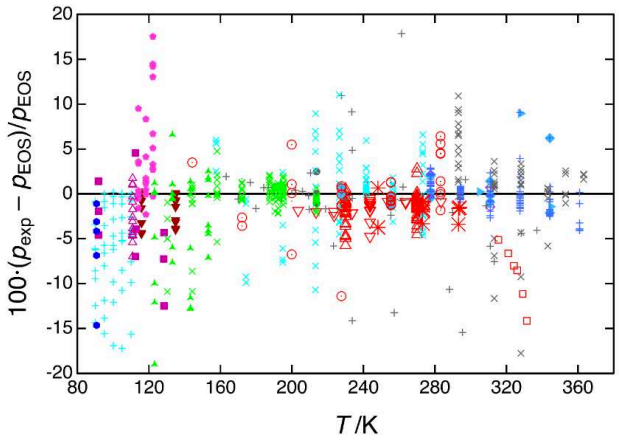

Figure 7: Methane and propane experimental saturation pressures (p_{exp}) compared to calculated saturation pressures (p_{EOS}) using the GERG-2008 equation of state of Kunz and Wagner[6]. Shown are several literature sources detailed by McLinden and Richter[7].

Although this system has several data sets with overlapping temperatures and compositions there are deviations from 10 % and up. This indicates that the method from which the data was collected can be improved. Current collection techniques require portions of the VLE sample to be removed in order to run through diagnostic instruments[8,9]. Due to this component of sample being separated, it is difficult to definitively determine the actual thermodynamic conditions that the sample is at during data collection.

Gas chromatography is also used in two studies that explored gas solubility of methane and water at low temperatures. Similar to SWRI, Frost et al.[8] and Mohammadi et al.[11], separated the desired portion of sample from the bulk sample in order to run it through a gas chromatograph. In these studies, the gas chromatograph was outfitted with a thermal conductivity detector (TCD), in addition to an flame ionization detector (FID), allowing it to detect concentrations of water. This water detection method is highly dependent on calibration in order to read correct water content.

A drawback of gas chromatography is the time required to calibrate each of the detectors in the system. Both Frost et al. and Mohammadi et al. describe that prior to each experiment calibration occurred for both the flame ionization detector and thermal conductivity detector.

Kim et al.[9] explored the solubility of methane in water at a variety of pressures but utilized methods that resulted in higher uncertainty than that of both Frost et al. and Mohammadi et al. The experimental method utilized was an indirect composition measurement. This technique was highly dependent on the accuracy of composition determination. Frost et al., Mohammadi et al. and Kim et al., together have measured a large range of pressures whose results follow a similar trend but have deviations upward of 10% (Figure 8).

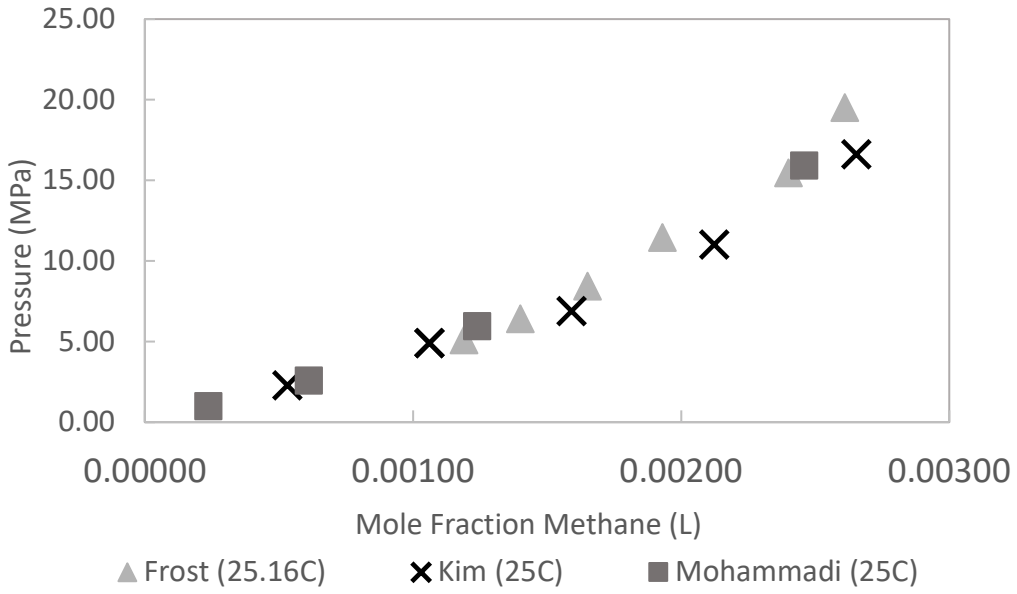

Figure 8: Frost et al.[8], Mohammadi et al.[11] and Kim et al.[9] compiled data for composition of dissolved methane in water at varying pressures.

Suiter et al.[12] have explored a new VLE data collection technique that does not require any portion of the sample to be removed in order to be analyzed like in a gas chromatograph. This method utilizes nuclear magnetic resonance (NMR) spectroscopy to collect the data. The use of NMR, in this preliminary study, yielded low uncertainty results without any need to calibrate the

composition measurements. Of course, the method was documented to have its drawbacks. Reported disadvantages are the control and measurement of temperature and pressure within the instrument. Therefore, with some development on the temperature and pressure measurement, this method would outperform the "standard" VLE measurement technique.

1.4. THESIS OBJECTIVE AND OUTLINE

Herein, NMR spectroscopy is used to do liquid phase measurements of VLE data for the system of methane and water to help improve the equation of state (EOS) solving software, NIST's REFPROP. Methods developed will be applicable to vapor phase measurements in future work.

The organization of the thesis is as follows:

Chapter 2 provides a brief overview of nuclear magnetic resonance (NMR) spectroscopy, including the advantages and disadvantages that come along with it. Following subsections discuss the possible measurement techniques for both liquid and vapor phases. Also discussed are possible pressure and temperature measurement challenges and techniques.

Chapter 3 describes the experimental methods starting with the NMR sample cells used with each of their characteristics. Additionally, this chapter describes how each sample was prepared, the method chosen for data collection, and discusses the VLE calculations in REFPROP.

Chapter 4 presents and discusses the experimental results for liquid phase equilibrium data collected and makes several comparisons to the calculated results in REFPROP.

Chapter 5 summarizes the outcomes of the study and gives ideas for future work.

2. BACKGROUND

2.1. NMR SPECTROSCOPY.

Nuclear magnetic resonance spectroscopy has been developed for more than 70 years in both scientific and medical applications (MRI - magnetic resonance imaging). This type of spectroscopy utilizes radio frequencies and a magnetic field to detect nuclear spins inside of the spectral window[15]. The spectral window is the small section of the NMR cell that is in the magnetic field (Figure 9).

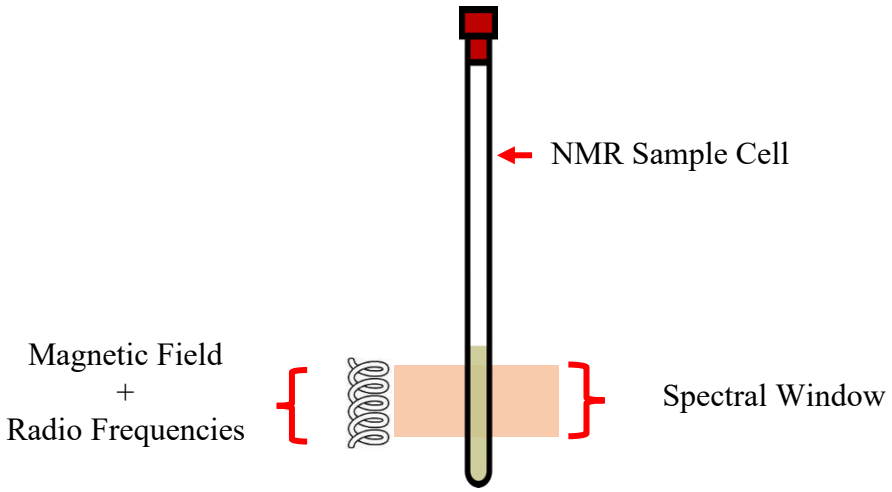

Figure 9: A fundamental look at the major components in an NMR experiment: Sample cell, spectral window, and the magnetic field.

There are two main configurations of NMR spectrometers; large high-field instruments and small medium-field (benchtop) instruments. The high-field NMR uses a large cryogenic superconducting magnet to produce a large and uniform magnetic field. This large magnetic field allows for higher resolution spectra, better sensitivity, and finer control on acquisition parameters. Alternatively, the benchtop instrument utilizes a smaller permanent magnet and a more user-friendly interface to collect data. This permits the instrument to be packaged inside a small

envelope while still allowing the user to take quality spectra. Each one of these instruments excels measuring different phases. The benchtop instrument handles large signals from highly protonated liquid phases better and the high-field instrument is able to better measure small vapor phase signals.

There are several different types of nuclei that are able to be detected inside an NMR instrument, but the most common for quantitative studies is ^{1}H. ^{1}H gives relatively large spectral signals and easy to implement parameters that lead to signal areas that are proportional to the number of nuclei in the sample (Figure 10).

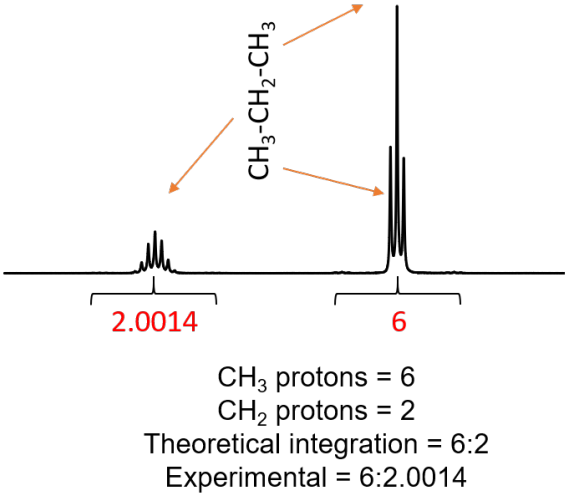

Figure 10: Propane spectrum with both theoretical and experimental integration.

An important characteristic of NMR is that it allows for direct determination of mole ratios inside the sample without calibration. In VLE experiments this in-situ composition measurement is precisely what is needed for high quality data.

The NMR instrument selection for this work was provided by NIST, National Institute of Standards and Technology. At the facility in Boulder Colorado, there are two NMR instruments available a Bruker 600 MHz and a Magritek Spinsolve 60 MHz (Figure 11).

Figure 11: (Left) Bruker high field 600 MHz NMR instrument[16]. (Right) Magritek Spinsolve 60 MHz NMR instrument[17].

Each of these instruments have advantages in their own regard. The high-field Bruker has the ability to manipulate the temperature of the sample cell via heated inert gas flow. This instrument also has an elevated sensitivity compared to the Magritek instrument. This is a result of the magnitude of the magnetic field and the manual user manipulation of the instrument. The benchtop instrument has a magnetic field that is a tenth of the Bruker instrument, giving it a limitation of sensitivity. In some scenarios this lower sensitivity is advantageous, for example when trying to measure highly protonated fluids (e.g., large water content). In the high field instrument the large signal would be excessively large potentially damaging the instrument's receiver. Each of these instruments are extremely capable and are complementary for this work.

2.2. ADVANTAGES AND DISADVANTAGES OF NMR.

NMR spectroscopy is an excellent experimental method in certain scenarios and carries with it many advantages. One advantage is its ability to capture data without physically removing

any portion from the bulk sample. This is extremely important when trying to take measurements of system equilibrium because the effect of removing part of the sample could alter the state at which data is taken from. Another advantage is the direct determination of composition (mole fraction) of each constituent in the mixture. This is a valuable attribute to NMR spectroscopy because of the high accuracy composition measurements that can be calculated from the spectra without calibration[12]. NMR also has the ability to detect very small concentrations less than 4 ppm[18]. This is valuable to improve the accuracy of the VLE experiment.

Some of the drawbacks of NMR spectroscopy are the ability to accurately determine the temperature and pressure that the sample is experiencing. With the large magnetic field, standard measurement techniques for temperature and pressure are heavily influenced, ultimately contributing to the entire experimental uncertainty. An additional drawback from this technique is the associated uncertainty that comes with overlapping signals. This overlap is prevalent in similar structured molecules in mixtures. The significance is the possibility of accounting for the overlapping signal in the wrong integration, leading to an incorrect concentration result. There are methods to numerically account for this overlap, yet this technique brings with it associated uncertainty. One additional limitation of NMR spectroscopy that adds to the difficulty of the high pressure VLE measurement is the cell material restrictions. Each NMR cell must be made of a non-magnetic material and be no more than 5 mm in diameter. With these design constraints, most commercially available NMR cells have a maximum pressure less than or equal to 2 MPa. There are a few solutions to this, one of which to make the cell out of a material that is non-magnetic and is stronger than glass. Daedalus Innovations[19] has developed a cell that is made out of zirconia, a high strength glass like ceramic with an integrated high strength aluminum needle valve (Figure 12).

Figure 12: This high-pressure cell is able to hold and maintain up to 100 MPa with its high strength ceramic construction and integrated needle valve[19].

2.3. LIQUID AND VAPOR MEASUREMENTS

The VLE measurement requires quantification of both liquid and vapor phases at thermodynamic equilibrium. This measurement of both phases can be done either simultaneously or separately. The characteristics of VLE makes conventional measurement methods not as successful as NMR spectroscopy. In NMR, phase composition can be determined while the sample is still experiencing its thermodynamic equilibrium.

There are several key experimental subtleties that go along with measuring both phases simultaneously. First, within the spectral window there must be a portion of each phase. There are multiple methods of orienting the sample to get both phases in the spectral window at the same time[12]. One method involves placing the instrument so that the meniscus of the liquid-vapor interface in the spectral window (Figure 13).

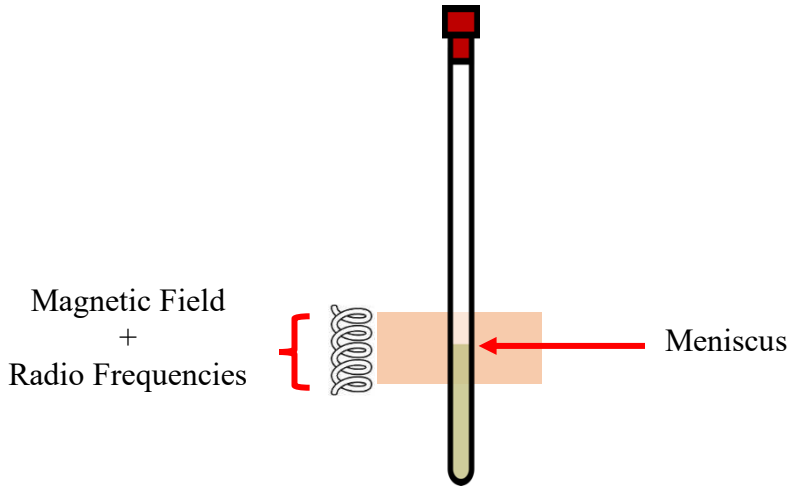

Figure 13: A visual representation of a possible technique of capturing both phases inside the active spectral window.

This method seems to be exactly what is needed; unfortunately, when there is a large density gradient in the spectral window (going from liquid to a vapor phase) undesired complications arise. This gradient in density results in a gradient in magnetic permeability[12], which is tedious to compensate for with the magnetic field (shimming). This shimming, in the end, only allows for one phase at a time to have proper peak shape to integrate (Figure 14).

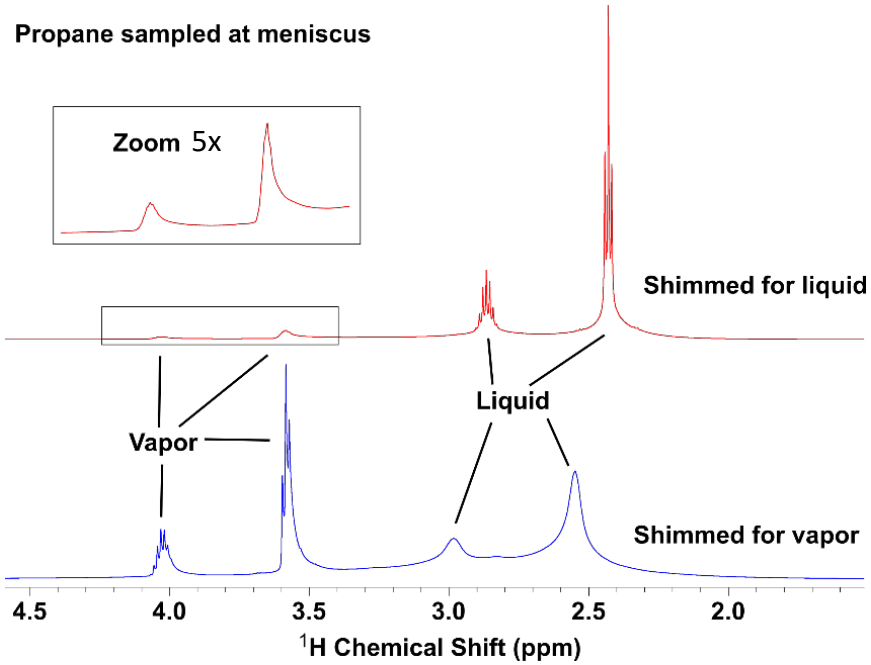

Figure 14: Two spectra of propane liquid and vapor both collected at 303 K. The sample cell was positioned such that the meniscus of the liquid vapor interface was in the active spectral window. Manual adjustments to the magnetic fields homogeneity (shimming) were done individually to each phase. Integration was not possible for all signals at the same time. Figure adapted from Suiter et. al.[12].

In order to measure the composition of both phases simultaneously a fundamental characteristic of liquids must be utilized, surface tension. To manipulate this property, a small reference fluid filled capillary tube must be placed inside the NMR cell, allowing for the liquid phase to be wicked up by the surface tension of the liquid. This liquid phase is drawn up between the capillary tube and the inside NMR cell wall[12]. This technique provides the NMR a nearly uniform phase composition through the length of the active region on the sample cell (Figure 15).

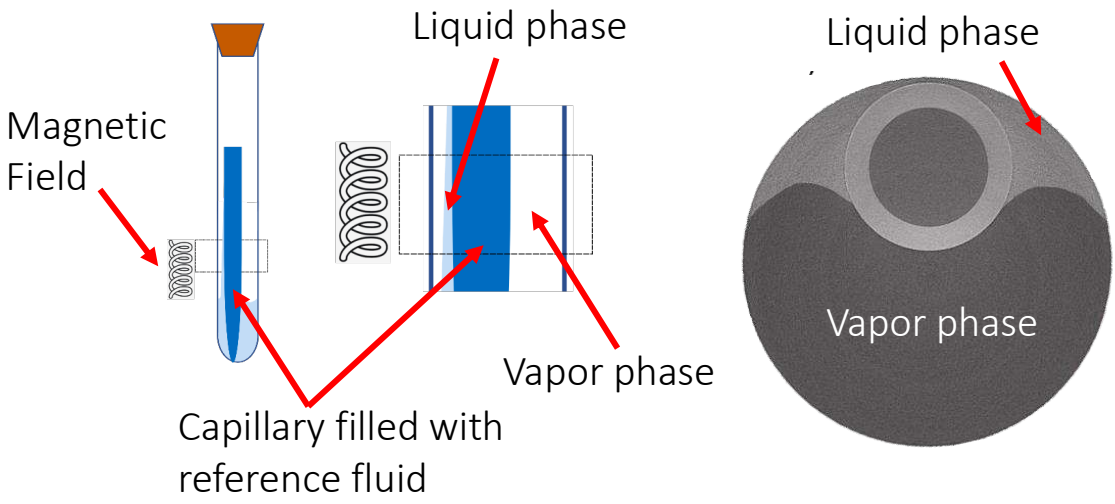

Figure 15: (Left) An NMR sample cell with a reference-fluid-filled capillary wicking up some liquid phase into the active spectral window. (Right) cross-section of the actual NMR cell with capillary and wicked liquid phase. Adapted from Suiter et al.[12].

This consistent composition throughout the active window allows for clean and defined spectra. The spectra would have five signal peaks; liquid and vapor phase signals of both constituents and the capillary reference signal.

The flame-sealed capillary has another function: to produce a signal intensity reference. This standard reference and its functionality are discussed in the following section.

Another approach for determining the composition is to measure each phase separately. One could adjust the height of the sample cell in order to capture a single phase inside the spectral window at a time. Unfortunately, this method is limited by the instrument's geometry and construction. In the case of the large instrument, there is not enough height adjustment in the location of the cell to get only one phase in the spectral window at a time. Instead, a new sample can be made to adjust the level of the liquid phase. Reproducing the sample with a different amount of liquid is heavily dependent on the sample preparation and the ability to control the temperature

and pressure of the cell. This approach of preparing a new sample for every data point is contingent upon accurate methods of measuring temperature and pressure.

2.4. PRESSURE CONTROL AND MEASUREMENT

One of the most important details that needs to be addressed in a VLE measurement is the pressure inside the cell at data collection. This reported pressure is extremely important for accurately describing the state of the mixture within an EOS software. Therefore, in order to compare the results from the experiment, there must be extremely low uncertainty pressure data for each measurement.

In traditional gas chromatography measurements, the pressure is directly measured from the bulk sample[8-11]. This is done through a calibrated pressure transducer closely connected to the large volume cell. In the case of NMR, this direct pressure measurement is not always possible because of a few characteristics of the instrument. When utilizing the high field NMR for VLE mixtures, connecting the cell to a pressure transducer is nearly impossible. Since the NMR is producing a large magnetic field, the transducer must be located far enough from the instrument in order to ensure the readings are not affected. Therefore, a long length of stainless-steel tubing is needed to properly separate the transducer from the NMR. A consequence of this large connection line in the actual experiment, is that the water vapor could condense inside due to lower tube temperatures above the sample cell. Such condensation would affect the pressure readings from the transducer, resulting in a systematic error. This condensation could also affect the VLE compositions measured due to the loss of water vapor from inside the sample cell.

Similar to pressure, from the standpoint of mixture model development, vapor phase density can be determined from the NMR spectrum. This indirect method can be done by utilizing an internal reference signal with an associated calibration curve. The internal standard signal can

be made from a reference-fluid-filled capillary within the sample cell, which gives a signal that does not change in intensity regardless of the pressure in the sample. To construct the calibration curve one normalizes the vapor signals by the reference signal by dividing the vapor signal area by the capillary signal area. Then the normalized peak area is plotted against the density of the vapor phase (normalized by the number of protons in the vapor phase) resulting in a linear calibration curve. This calibration curve can then be utilized to determine the vapor phase density of a closed cell by using that same capillary during data collection[12] (described in more detail in Section 4.2.1). This method is reliant on the capillary signal not overlapping any of the signals of the sample.

Pressure control is as important as pressure measurement. There are a few types of pressure control techniques that can be implemented in an NMR experiment. Depending on the sample cell that is used, one of the most common techniques is to simply regulate the pressure from the source and seal off the cell with a valve. This method is dependent on the sample cell having an integrated valve to close the cell off. It also relies on the cell being able to hold pressure for an extended period of time. Another method of pressure control is where the cell is connected to the gas source for the entire duration of the experiment. The gas source could either be a gas bottle with regulator or a pump. Unfortunately, during an actual VLE experiment the direct pressure control would likely lead to condensation in the long section of tubing.

2.5. TEMPERATURE CONTROL AND MEASUREMTENT

Temperature control and measurements are also vital in VLE measurements and modeling. Of the two, temperature control is dependent on the type of instrument. For example, the high field NMR is equipped with a heated inert gas that flows over the cell to heat it to the desired temperature. It is not practical to change the sample temperature in the benchtop instrument, its

permanent magnet requires a constant temperature. Both cases require a method of measuring the actual sample temperature with an additional temperature probe to ensure the accuracy of the internal readout.

Similar difficulties to measuring pressure arise when trying to measure the temperature of the NMR sample. The instrument's high magnetic field affects most standard temperature probes. One temperature probe that is specifically designed for high magnetic fields and low cryogenic temperatures is a Cernox[22] thermometer. A temperature probe of this type was used and was calibrated with two fixed point cells: gallium melting point and water triple point.

An indirect method of determining the temperature within the sample is by the relative peak positions for a standard. Most common fluid for this is deuterated methanol, which has two distinct peaks. The peaks separation distance (in hertz or ppm) can be used to calculate the temperature of the methanol within about one degree Celsius of accuracy[20,21] (Figure 16).

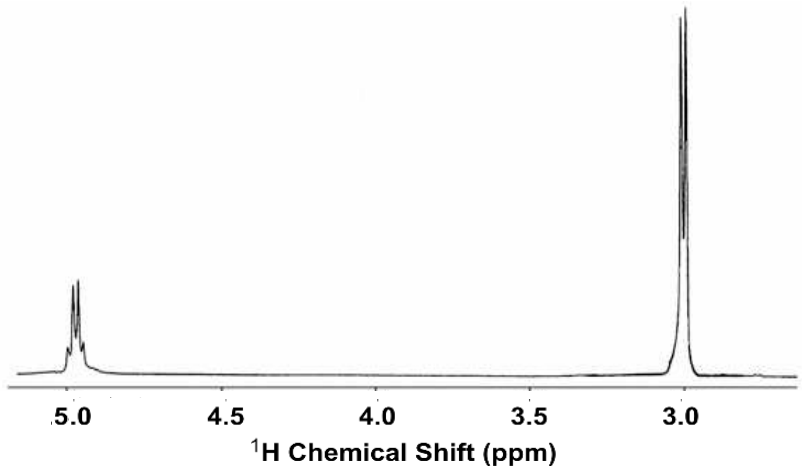

Figure 16: Spectrum of deuterated methanol at -20°C. As the temperature is varied the distance between the two peaks will be directly affected[20].

This method can be implemented in a similar manner as the reference signal capillary for determining pressure. Experimentally, a capillary filled with deuterated methanol is placed inside the sample tube. When the experiment is done, the spectrum will have both methanol signals and

VLE signals. One subtlety with this technique is that the accuracy of the resulting temperature is dependent on the signals from the methanol and VLE data. This means that it will only work when there is no overlap on these two methanol signals, limiting the systems that this will work for. This could also be done prior to the actual VLE experiment with only the deuterated methanol inside the sample cell to determine the average temperature in the spectral window.

3. EXPERIMENTAL AND COMPUTATIONAL METHODS

3.1. INSTRUMENT SELECTION

After several preliminary studies of the capabilities of each instrument, a methodology on data collection was chosen. In this work both benchtop and high field instruments are utilized. The benchtop system proved to not be able to detect water vapor due to the limitations of sensitivity or shimming procedure (Figure 17).

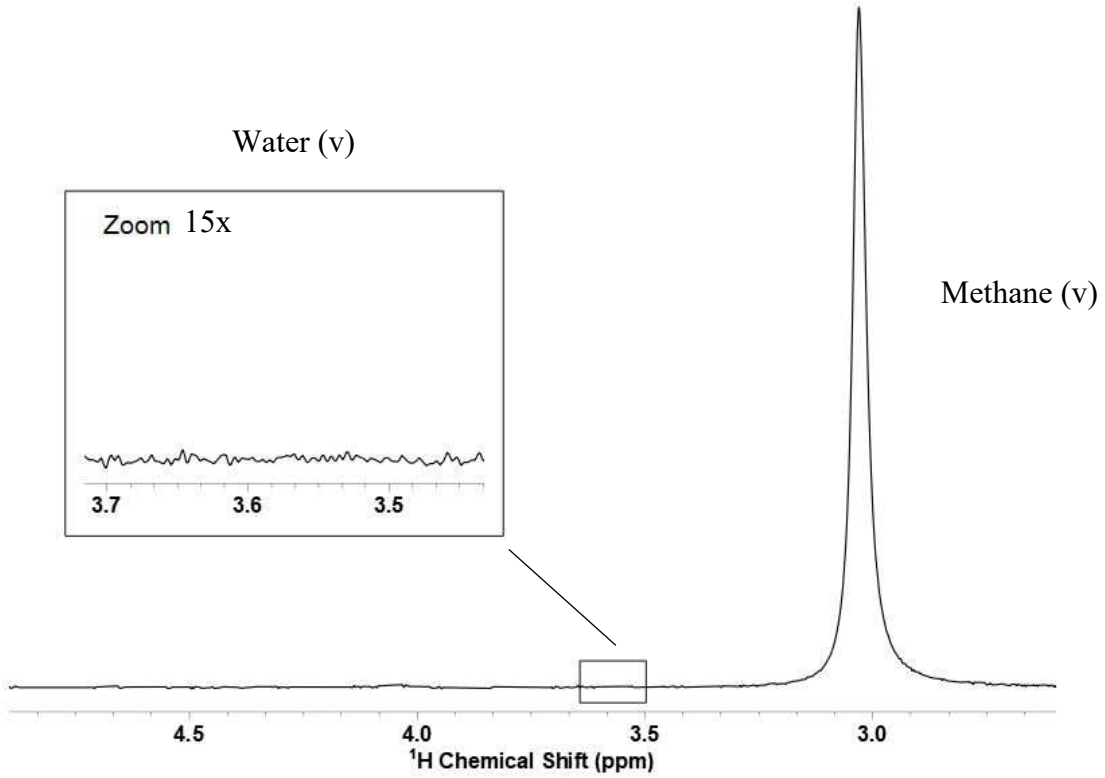

Figure 17: Spectrum of H_2O and methane at 1.03 MPa on benchtop instrument. There were no traces of water vapor in the spectra taken. Also, with the fixed temperature instrument, there are not a large number of options to definitively determine the peak identity.

This prompted a switch to the high-field instrument due its higher sensitivity. With some initial tests it was determined that the high-field instrument was able to detect and resolve water vapor (Figure 18).

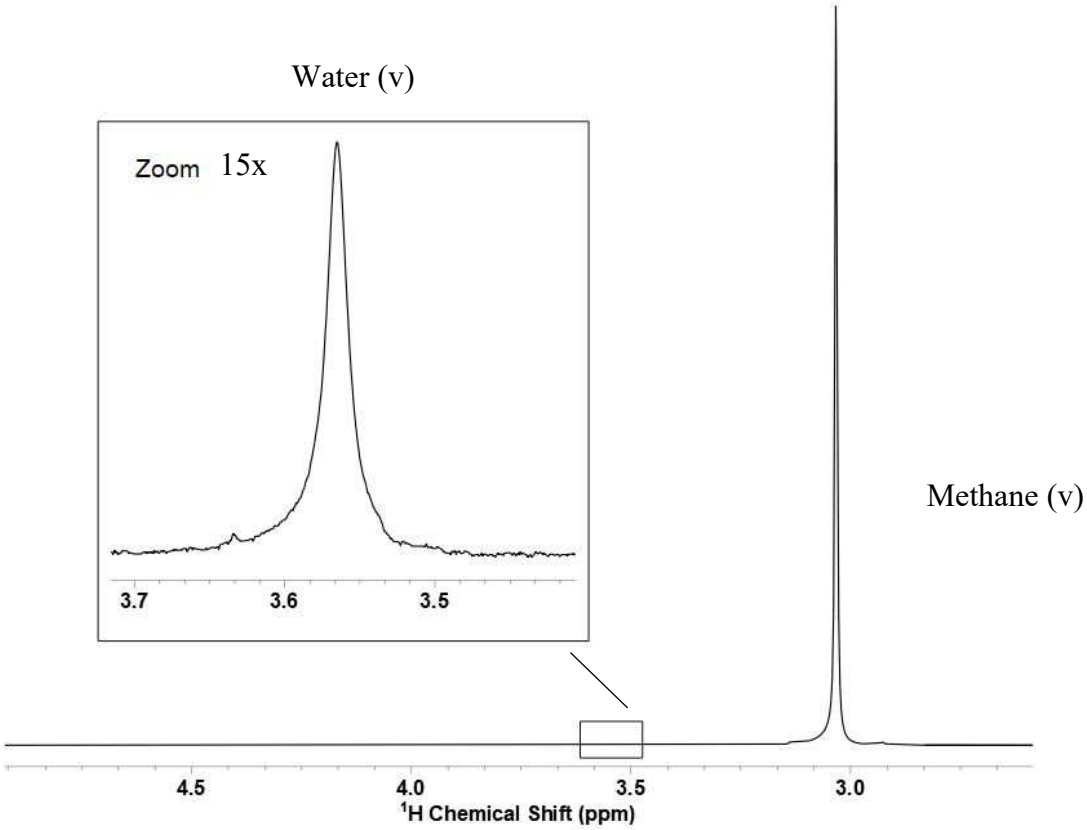

Figure 18: High-field instrument water vapor detection of a sample with small amount of H_2O and methane pressurized to 1.03 MPa. This was determined to be water vapor due to the variation in signal strength with increasing temperature.

Initial tests, which were designed to determine if both phases could be measured in the same spectra, were not successful. Unfortunately, due to the capillary signal and the composition of the system (methane and water) there were unavoidable peak overlaps in the system (Figure 19).

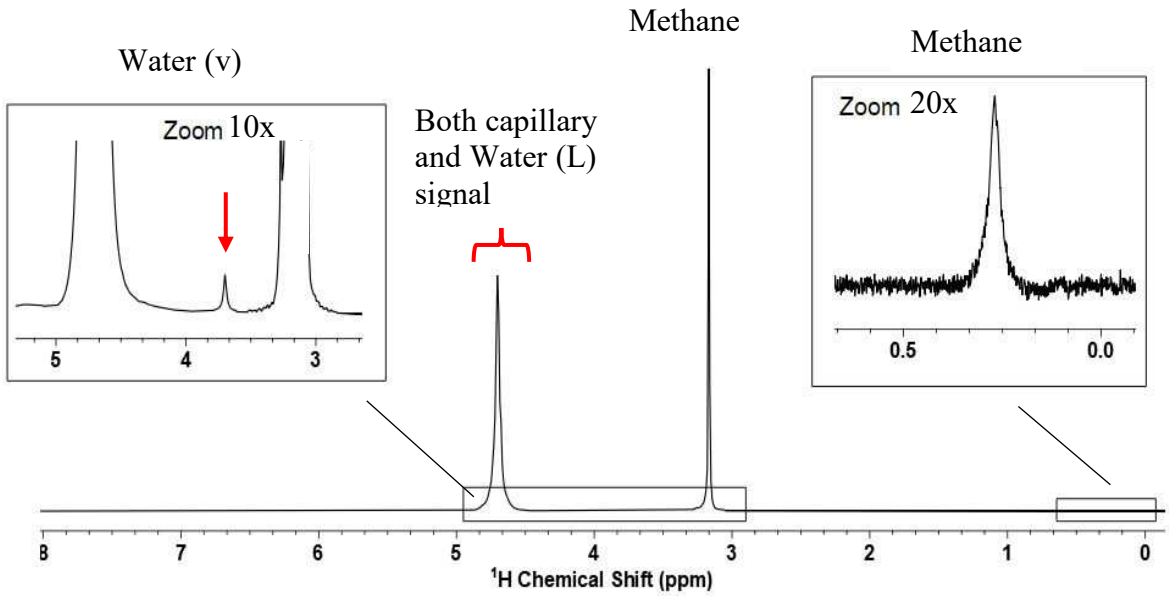

Figure 19: Spectrum of a mixture of D_2O and water pressurized with methane at 1.03 MPa at 45°C with a D_2O filled capillary. Note that the signal from the water is overlapping completely the signal that is coming from the capillary.

After using D_2O as a reference fluid in the capillary and not being successful on detecting all expected signals (methane liquid/vapor + Water liquid/vapor + capillary signal) several substitutes for D_2O were used. The tested fluids were chloroform, benzene, and methanol. Similar outcomes were observed with these three additional reference fluids with some overlap in the system. An additional NMR technique was used to offset the natural chemical shift of the capillary signal. The method was to add 0.5 millimolar of gadolinium chloride ($GdCl_3$) to the capillary. The $GdCl_3$ did not shift the signal enough to integrate all signals. This ultimately did not allow for simultaneous determination of both phases.

With all of these preliminary tests completed, the methodology chosen for this work was to split up the measurements between both instruments for both liquid and vapor phases. In this work we focused on the development of measurement methods for the liquid and vapor phases and actual data collection of only the liquid phase.

3.2. TEMPERATURE AND PRESSURE MEASUREMENT METHODS

Two different methods were used to determine pressure depending on the phase measured. For the vapor phase measurement, the vapor phase density calibration curve and the reference-fluid capillary signal were utilized (Section 3.5). This method was chosen due to no significant peak overlap in any of the three signals. For the liquid phase measurement, the pressure was measured with a pressure transducer prior to sealing the sample with the integrated needle valve on the sample cell. This method was ultimately chosen after conducting several pressure repeatability studies (See Section 4.1.1.).

Measuring sample temperature in each instrument was completed using the same temperature probe. Finding a temperature probe whose signal is not affected by the large magnetic field on either of the instruments was a challenge. The probe that we ultimately chose was the Lakeshore Cryotronics Cernox AA temperature probe. This probe, described by the Lakeshore Cryotronics, is "…resistant to magnetic-field induced errors…"[22]. With this temperature probe selected, a few fixed-point temperature calibrations were conducted (See Section 4.1.2.).

3.3. NMR SAMPLE CELLS

Throughout this work two different types of NMR cells were utilized to perform VLE measurements. We utilized two cells because the high-field instrument was not able to run 100% H_2O, ultimately requiring the use of the benchtop instrument. Each NMR spectrometer requires a different type of NMR cell. Starting with the benchtop instrument and its low-pressure liquid phase measurements, we used a 7-inch Willmad Lab glass NMR tube. This sample cell has an integrated PTFE needle valve (Figure 20).

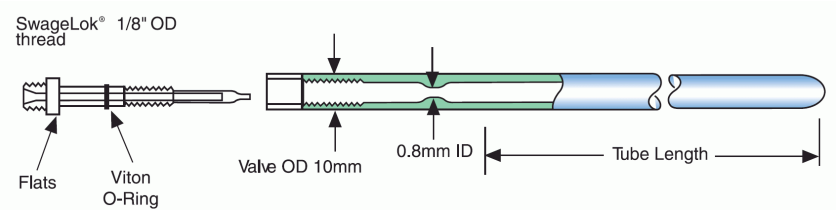

Figure 20: Willmad Lab Pyrex® sample cell with integrated needle PTFE valve[23].

This sample cell, made from Pyrex® glass, has an outer diameter of 5.0 mm and an internal diameter of 3.6 mm. This cell has a PTFE integrated valve at the top of the sample tube that also contains an 1/8-inch Swagelok fitting to connect the cell to control the pressure. The cell is rated to 2.068 MPa (300 psig), slightly under 1/3 of the targeted 6.9 MPa (1000 psig). In order to reach these elevated pressures another sample cell was utilized in the high field NMR.

The Daedalus Innovations high pressure NMR cell allows for internal pressures to reach up to 100 MPa (14,500 psig). This NMR cell is constructed out of zirconia, a high strength ceramic. Similar to the glass NMR cell that was utilized in the benchtop instrument, this cell has an outer diameter of 5.0 mm. The internal diameter is 3.6 mm, and the cell has an integrated needle valve on the cell manifold made from 7068 aluminum (Figure 21)

Figure 21: Daedalus Innovation's high-pressure zirconia sample cell (top)[19]. High strength 7068 aluminum manifold with integrated needle valve (bottom). The scale is in millimeters.

The cell's integrated needle valve has been tested by Daedalus Innovations to reveal that a sample can be pressurized, sealed, and can maintain pressure for months[19]. An additional high-pressure manifold was designed and manufactured to allow for direct 1/16th inch Swagelok connection while lowered into the high field NMR. The decision to design and manufacture a new manifold came after testing the existing one in the large instrument. The existing manifold had its high-pressure connection located on its side, ultimately not allowing for the transfer line to be attached while inside the instrument. The new high-pressure manifold that allows for direct pressure measurements can be seen in Figure 22.

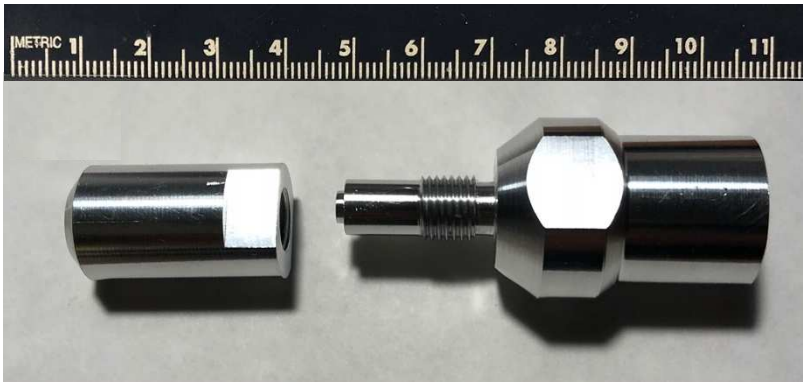

Figure 22: New high-pressure manifold, manufactured out of 7075 aluminum with ¼ inch NPT threads instead of a needle valve like the manifold from Daedalus. Scale is in millimeters.

This new NMR manifold is made from 7075 aluminum and was manufactured at CSU. The purpose of the new direct connection manifold is to take direct pressure measurements during the vapor phase density calibration (See Section 4.2.1.).

3.4. SAMPLE PREPERATION

Each sample was prepared using the same method regardless of which instrument the cell was to be measured with. Initially, each sample cell was connected to a manifold that allowed for the cell to be connected to both pressure regulator and mechanical pump. The cell was then evacuated with the mechanical pump (Marathon Electric ¾ HP) prior to filling it with any liquid.

The liquid was 90% D_2O and 10% H_2O in the high-pressure cell and only H_2O in the low-pressure cell. When preparing the high-pressure cell the concentration was gravimetrically measured out using a Mettler Toledo balance with calibrated accuracy of 0.1 mg. After the cell was filled with liquid, the sample was de-gassed with the same evacuation process as before. Throughout this process the cell was quickly tapped on the side of the cell to ensure that the formation of bubbles would not carry any liquid up and out of the cell. Once completely de-gassed, the sample cell was lowered into water filled dewar. The temperature in the dewar was controlled with a water circulation bath (Thermo Neslab RTE). The temperature in the dewar was set to match the NMR experiment. After placement in the water bath, with the sample still connected to the vacuum pump, a small amount of methane was pressurized on top. A few seconds later the vacuum pump was closed off and the cell was brought to pressure gradually over 5 min. Once at the desired pressure, the sample was let to sit for an additional 5 min to account for any drift in the pressure measurement. Then the sample was sealed off from the gas cylinder. Once sealed off, the sample was shaken to force the liquid to the top of the cell, then forced to return to the bottom (See Section 4.1.3. for details). This was completed three times, then the cell was returned to the water bath until it was time to run the sample in the NMR. This process was repeated for every sample for every data point.

When measuring the vapor phase, a sealed capillary is placed in the cell with the mixture to produce a signal that does not change (reference signal). This capillary is about 60 mm in length and 1 mm in outer diameter (Figure 23).

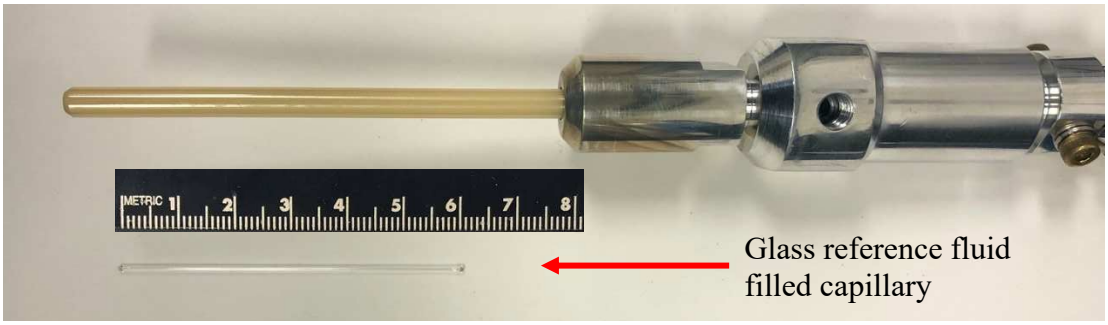

Figure 23: High pressure cell (Top) in comparison to the glass flame sealed capillary. Scale is in millimeters.

The capillary is first sealed with a butane torch on one end. From here the reference fluid of choice is injected inside the capillary with a syringe. The reference fluid is most commonly deuterated water (D_2O, 99.96 % deuterated). This deuterated water produces a signal that is very small in magnitude compared to normal water. Deuterated water achieves this small signal by having no protons within the hydrogen atoms (isotope of hydrogen).

3.5. VAPOR PHASE DENSITY

Compared to pressure, vapor phase density has a similar utility from a mixture modeling standpoint. Recalling the characteristics of NMR spectroscopy, the signal integration is directly proportional to the molar concentration of the sample. This fundamental principle of NMR can be applied to measure the molar density of the vapor phase. As mentioned in section 2.5, a calibration curve can be constructed by using a sealed capillary that is filled with a reference fluid. The calibration relies on the constant intensity of the reference signal from the capillary.

3.5.1. VAPOR PHASE DENSITY CALIBRATION

The calibration used here requires a reference-fluid-filled capillary be placed inside the NMR cell. For this work, deuterium (99.96% pure D_2O) was used to produce the constant reference signal. The capillary then was placed inside the high-pressure zirconia cell and held in the high-pressure manifold that allows for direct pressure measurement (described in section 3.2). This new

manifold allowed for the direct pressure measurement of the cell while inside the high-field NMR instrument. The high-pressure cell was connected to a pressure transducer (Paroscientific) with a range of 0-6.89 MPa and a compressed bottle of regulated methane from Matheson Gas Products by 2 meters of $1/16^{th}$ inch stainless steel Swagelok tubing. This assembly of the high-pressure cell and connection line was lowered inside the Bruker NMR instrument. This setup allowed for the pressure of the cell be manipulated and measured from outside of the instrument. The calibration was conducted with methane pressurized from 0 to 5.51 MPa and temperatures from 30°C to 70°C.

3.6. REFPROP VLE CALCULATIONS

REFPROP, like most equation of state solving software, requires several parameters to be defined to solve for a given system. For mixture VLE calculations, compositional and thermodynamic inputs are required. In this work, the parameters that were needed to make these calculations were the constituents of the mixture, the temperature and the pressure. The procedure that was used started with defining the mixture by choosing the constituents from the internal fluid database. After defining the mixture with in the REFPROP software, the calculation was made through the "Saturation tables" menu. From there two calculation variations were chosen "Vapor at dewpoint with coexisting liquid" and "composition at fixed T". This method was used to produce predictions of the equilibrium compositions of both liquid and vapor phases[24]. The liquid phase methane prediction (Figure 24) helps visualize the expected trend, that with larger pressures more methane will be dissolved in the liquid water. The vapor phase prediction reveals an opposite trend, that at lower pressures the larger concentrations of water vapor are predicted (Figure 25).

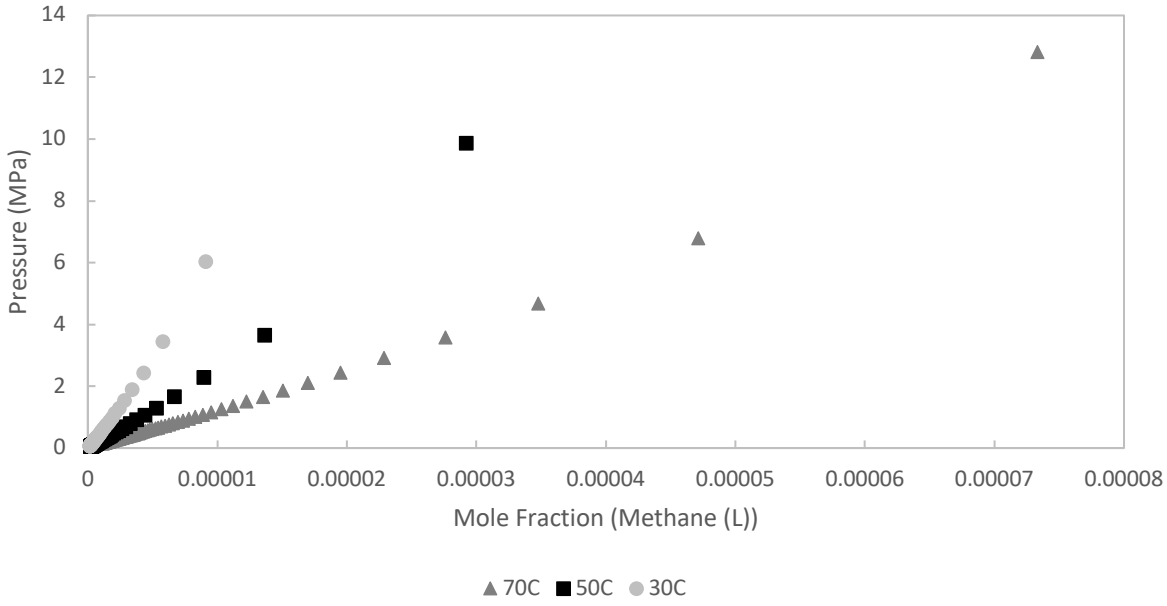

Figure 24: REFPROP prediction for equilibrium compositions of liquid phase methane from 30°C to 70°C of the mixture water and methane.

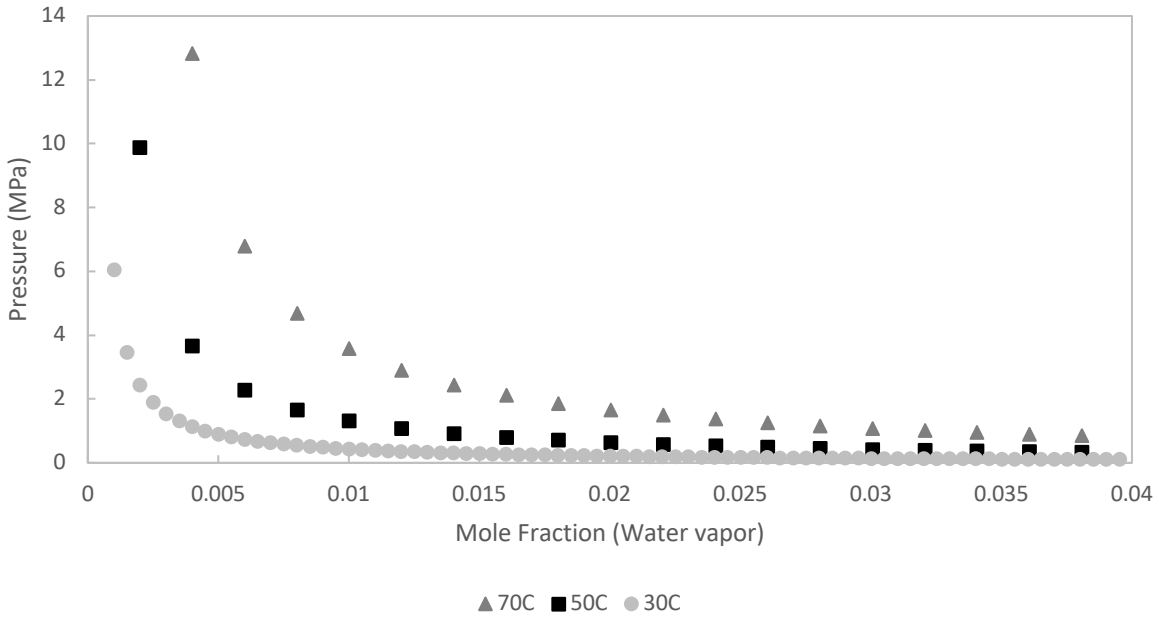

Figure 25: REFPROP prediction for equilibrium compositions of vapor-phase water from 30°C to 70°C of the mixture water and methane.

4. RESULTS AND DISCUSSION

4.1. LIQUID PHASE MEASUREMENT

The liquid phase measurement in this work was done by utilizing both NMR instruments to take full advantage of each of their discussed capabilities (Section 3.1). The Magritek Spinsolve benchtop instrument was used for data collection at low pressures with the Pyrex® glass cell (Section 3.2.) limiting the max pressure to 2.068 MPa. The benchtop instrument was auto shimmed using Magritek's optimized shimming routine (Power Shim) prior to each data point using the recommended 5 % D_2O + 95% H_2O mole fraction fluid (this sample was made by the manufacturer and included with the instrument). Once the sample was placed inside the instrument an additional sample shimming protocol was performed (Sample Shim) for each data point. Figure 26 shows a spectrum for the mixture methane + water at 1.72 MPa, which shows symmetrical peak shapes, narrow line widths, and the size difference between the two signals.

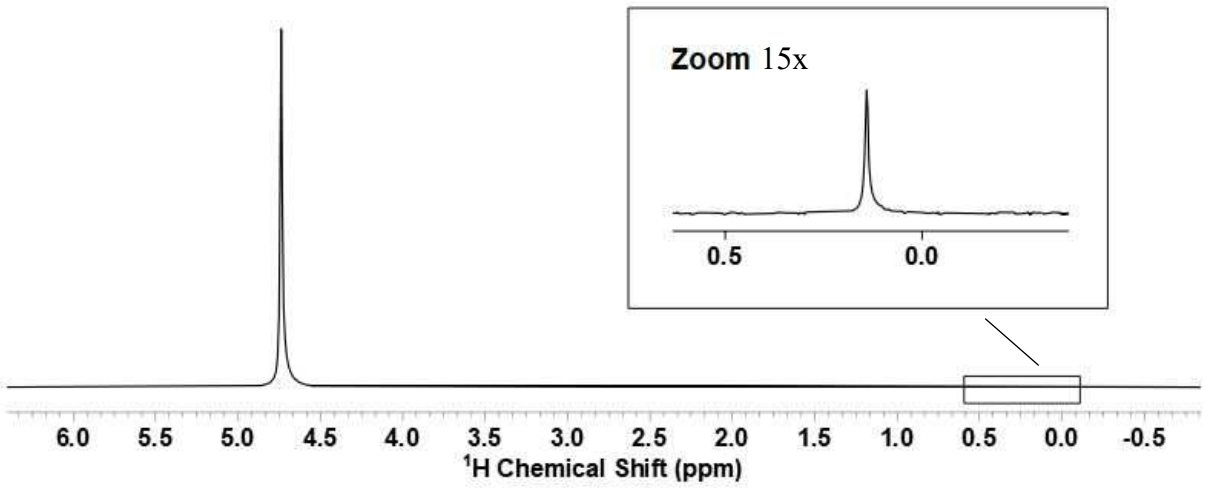

Figure 26: Spectrum taken of H_2O and methane at 1.72 MPa on the benchtop NMR spectrometer.

The second component to this liquid phase measurement was completed on the high field Bruker NMR instrument. This instrument in conjunction with the high-pressure zirconia cell extended our pressure range up to 12 MPa (limited by pressure regulator on methane cylinder 12MPa). The samples were lowered into the instrument and an automated shimming routine was performed for each data point. This shimming function was able to be utilized because of the deuterium component in the liquid phase sample mixture (10% H_2O and 90% D_2O) (Section 3.4). This shimming routine was able to produce high quality accurate spectra of the mixture (Figure 27).

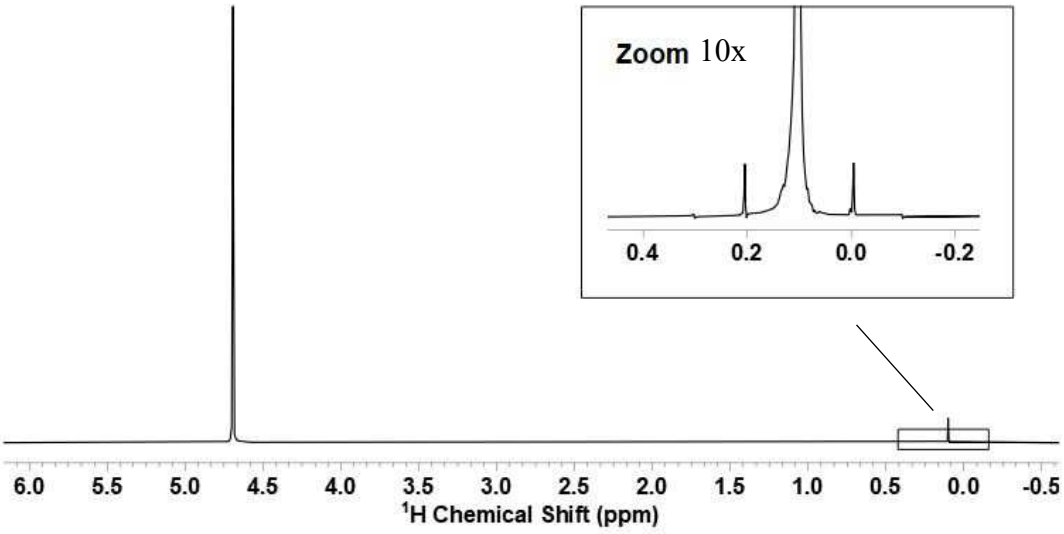

Figure 27: Spectrum of methane and 10% H_2O and 90% D_2O at 12 MPa. This was taken in the high-field instrument.

4.1.1. PRESSURE

Pressure measurement and control were one of the reoccurring challenges in this work. Due to the system characteristics, the method of manually setting the pressure of each sample and sealing it were unavoidable for liquid phase measurement. This method was chosen after running

several pressure studies on the repeatability of sealing the Daedalus Innovations high pressure cell with the same pressure (Figure 28).

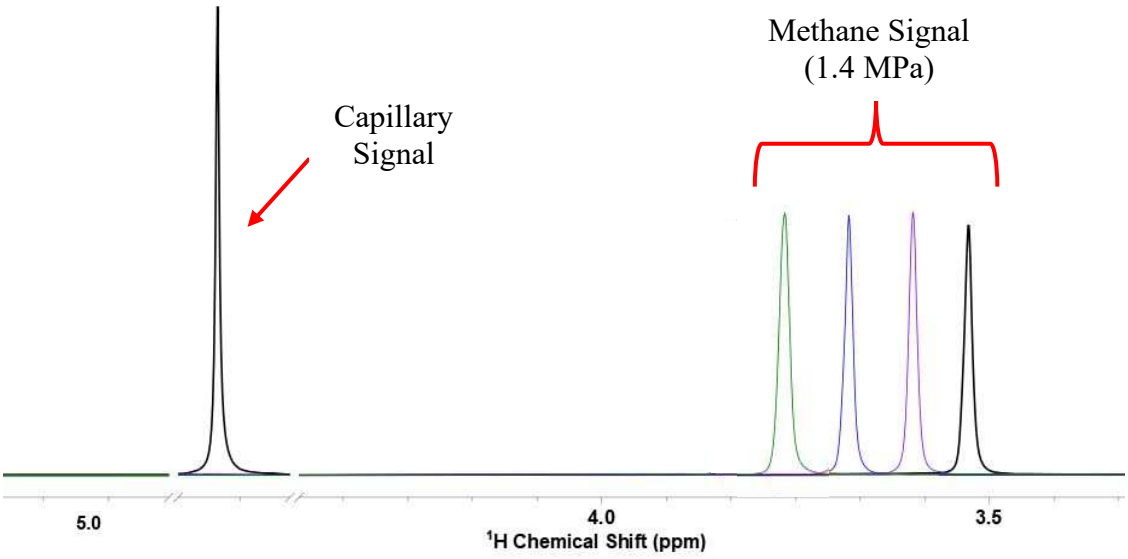

Figure 28: Composite spectra of narrow capillary with 50% H_2O and 50% D_2O (left) and 4 signals from independent re-pressurization of methane at 1.4 MPa (right). Each sample was pressurized and sealed to test the repeatability of this sample preparation. All capillary signals were normalized to the same signal intensity.

This preliminary study demonstrated the repeatability of this pressurization technique. The standard deviation from the methane signal, when normalizing the capillary signal was 2.937 %, (not including the second data point that was not evacuated prior to pressurization).

4.1.2. TEMPERATURE

Temperature measurement and control were measured inside of both benchtop and high field instruments prior to the experimental data set. First the probe was calibrated with a gallium melting point cell (302.9146 K), a water triple point cell (273.16 K), and a constant temperature water bath. The water bath had a calibrated platinum resistance thermometer inside along with the Cernox® probe. The reason for these additional points in the water bath is the non-linear nature of

the Cernox® probes resistance response. In the probe's manual the response form was reported to follow a power function. The calibration curve exhibits an excellent correlation between the curve fit and the calibration points (Figure 29).

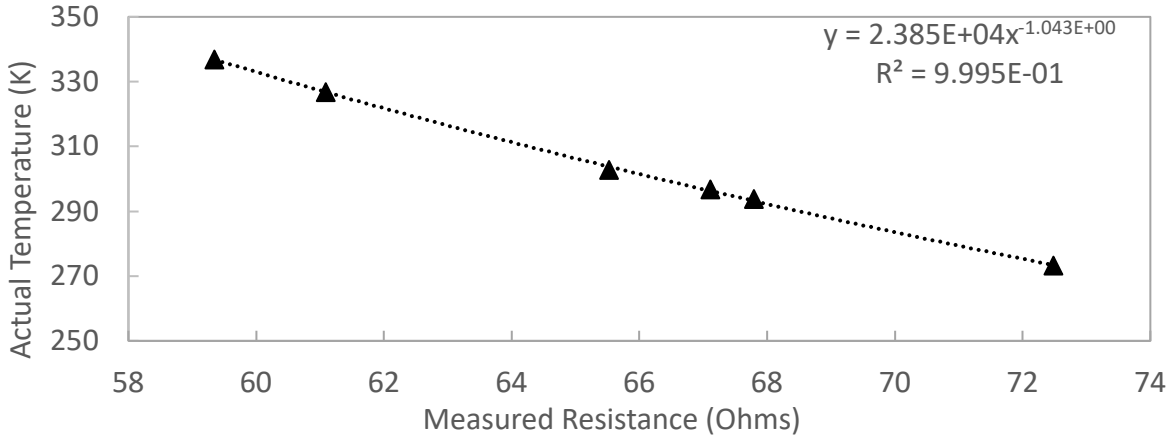

Figure 29: Calibration curve for Cernox® temperature probe, included are two fixed point cell temperatures and four water bath points that were verified with a platinum resistance thermometer.

Each instrument's spectral window temperature profile was measured with this Cernox® temperature probe. The benchtop instrument produced an average spectral window temperature of 26.5 °C with little gradient (Figure 30). Note the data points separation is due to the physical size of the probe, which ultimately limited the resolution of the profile.

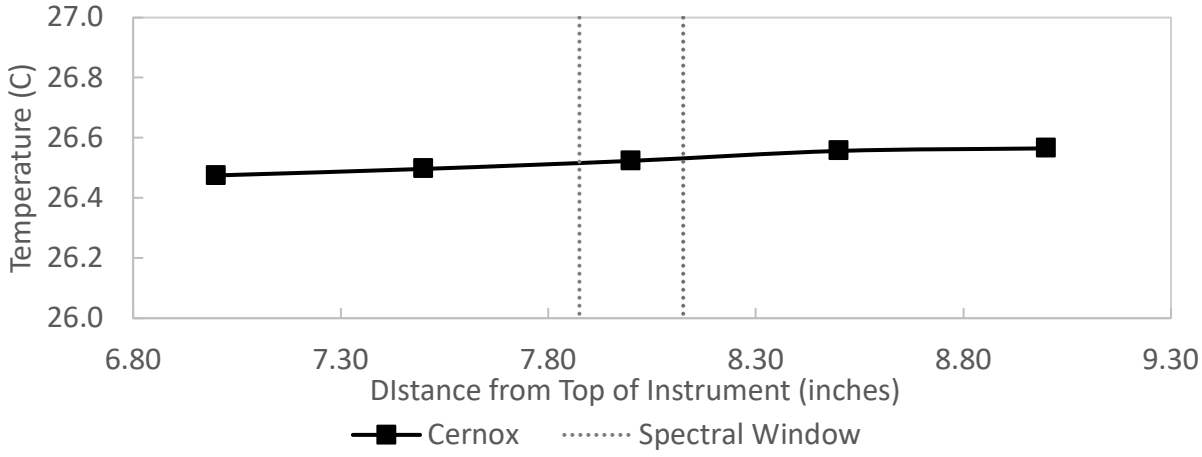

Figure 30: The temperature profile of the benchtop instrument with the calibrated Cernox® temperature probe, highlighted are the bounds of the spectral window.

The high-field NMR instrument has the functionality of adjusting the temperature of the cell. Temperature gradients were measured at three different set temperature: 30°C, 50°C, and 70°C. As measured by the Cernox® probe revealed at all three set temperatures the measured temperature was always a few degrees lower than the setpoint (Figure 31).

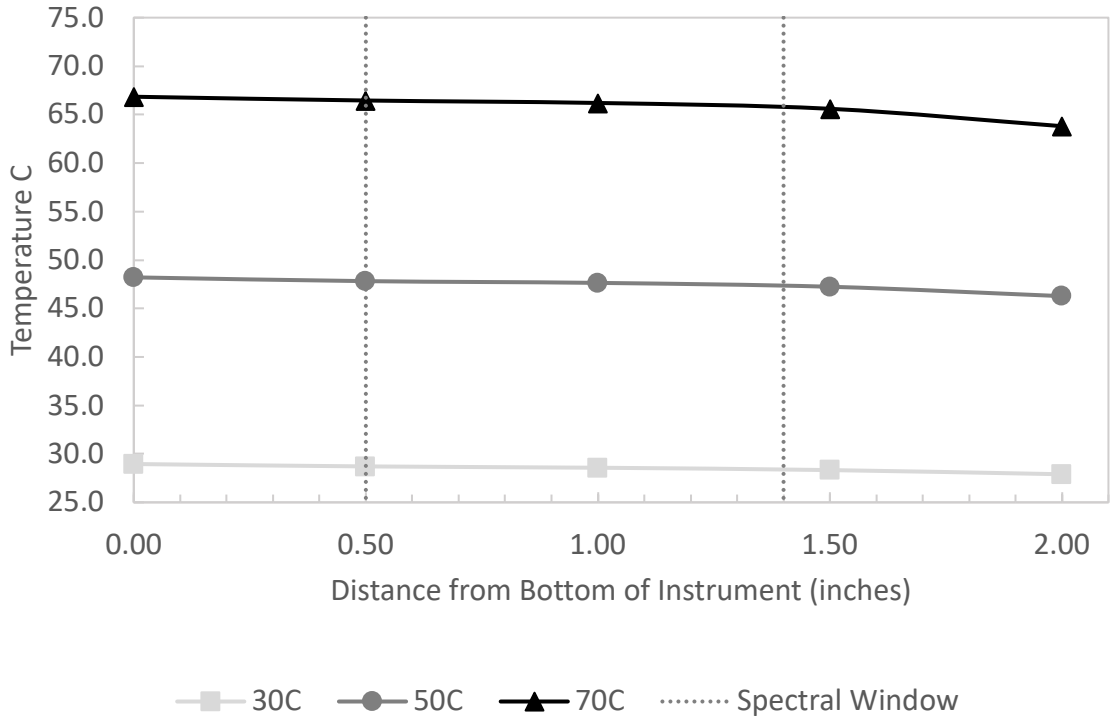

Figure 31: Temperature profile within the high field NMR at three different set temperatures 30°C, 50°C, and 70°C. Dotted lines represent the spectral window.

Both measurements demonstrate the low temperature gradients in both instruments and confirm that there are deviations in the large instrument's set temperature compared to actual. Prior to the experiment on the large instrument the temperature was measured, and the heating parameters were adjusted to get the exact desired temperature.

4.1.3. THERMODYNAMIC EQUILIBRIUM

An excellent characteristic of NMR spectroscopy is the ability to not remove any portion of the sample and still acquire compositional data from it. To determine when the sample has achieved equilibrium the composition must be measured over a period of time. Once the liquid phase composition of the sample stops changing with time, the sample is at equilibrium. Initial results show that a sample with methane and water at 1.72 MPa requires roughly three days to come to equilibrium. This equilibrium can be seen on Figure 32 as the "Not Shaken" data plateaus in composition after 3000 min. With only one high-pressure cell, this equilibration time was not feasible to complete the measurements. Therefore, we ran this equilibration time test a second time but agitating the sample after one initial scan. The results are that the sample comes to equilibrium nearly instantaneously after the sample is agitated (Figure 32).

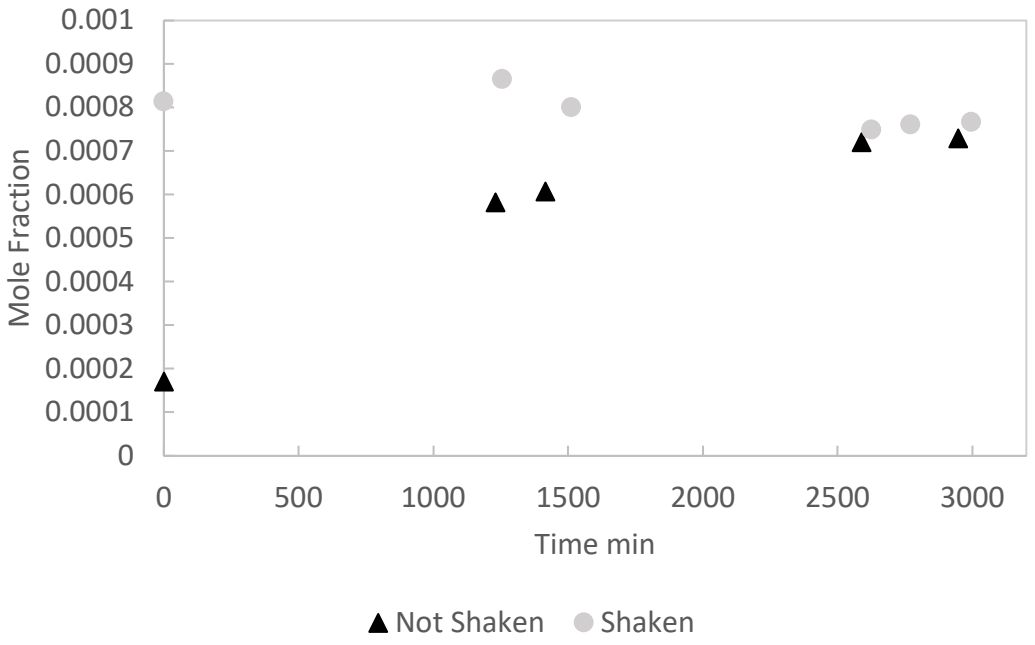

Figure 32: Equilibration trial inside glass Willmad Lab NMR cells with 100% D_2O at 1.72 MPa both shaken and not shaken.

By agitating the sample the total time from making the sample to running it through the instrument is 0.5 hours. This equilibration study was initially done only with the glass cells in the benchtop instrument. Later, when data collection started for the high-field instrument, it was observed that the samples did not equilibrate immediately after agitation, as judged by a continued increase in dissolved methane detected over 3.5 days (Figure 33).

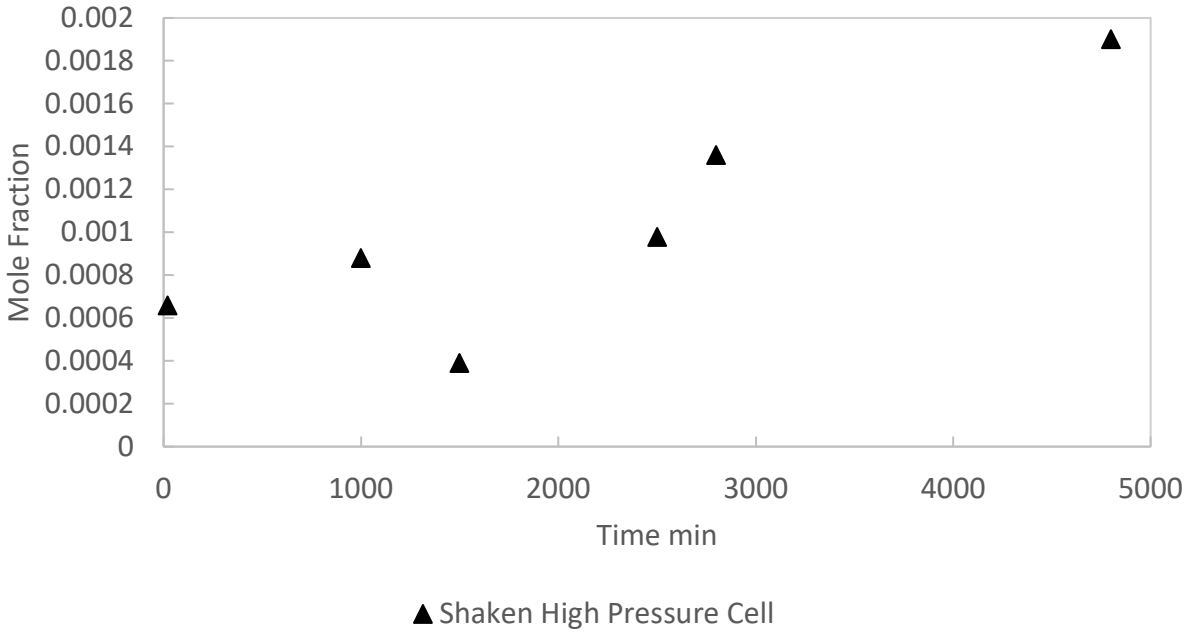

Figure 33: Measured dissolved methane in 90% D_2O and 10% H_2O on the high field instrument after sample was shaken at 12 MPa. Notice the different response of the measured methane content compared to that of the benchtop equilibration test.

This extended equilibration time on the large instrument suggests that the different cells promote different equilibration scales. Another possible reason for this difference in equilibration time is the higher pressures that the high-field instrument was run on compared to the benchtop instrument. Another source of this difference seen in Figure 34 is the internal geometry of each of the two cells utilized. The glass cell has a large empty volume at the top of the cell (Figure 34) which significantly increases the surface area of liquid exposed to the vapor phase.

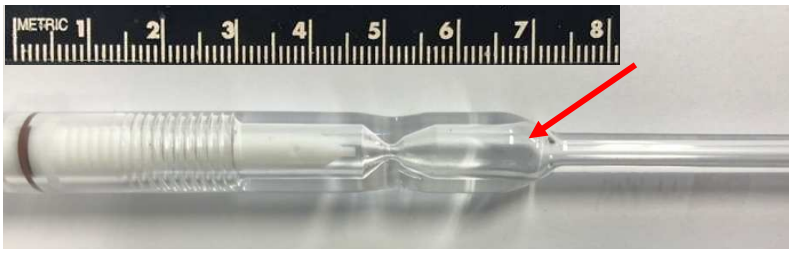

Figure 34: Glass cell with the open volume pointed out.

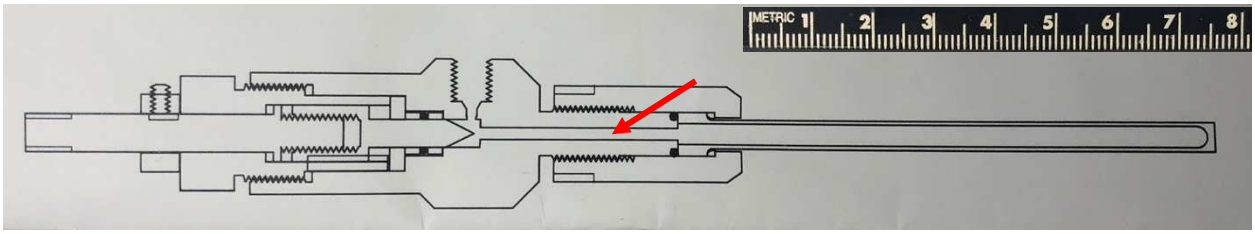

Figure 35: Cross-sectional view of the integrated needle valve and zirconia cell, pointing out the smaller diameter that is connected to the cell.

The high-pressure zirconia cell, however, does not have any large open volume at the top of the cell to help this exchange between phases (Figure 35). After measuring this difference, our plan shifted from preparing the samples for each instrument identically, to agitating the high-pressure cell four times more than that of the glass cell.

4.2. VAPOR PHASE MEASUREMENT PLAN

In this work, the vapor phase measurement was planned but not executed due to lab time limitations. The same temperature measurement method as described in the liquid phase section is planned to be used within the vapor phase measurements. The experimental procedure planned, requires the use of the high field Bruker NMR instrument and the high-pressure zirconia cell with a reference fluid filled capillary. The purpose of the capillary, in this case, is only for the vapor phase density measurement. The capillary will be centered in the tube to avoid the wicking described previously (Section 2.3). The vapor phase density calibration was completed in order to

fully understand and to develop an accurate plan to complete the vapor phase data collection in future work.

4.2.1. VAPOR DENSITY

To measure the vapor phase density a set of calibration curves were made. The reference fluid within the capillary provided a standard signal to compare against. The calibration curves were made by collecting a spectrum of a sample that had a gas at a known density with a reference fluid filled capillary inside the cell. The gas calibrant used was methane and the reference fluid inside the capillary was D_2O. Using the high-pressure zirconia cell, held in the new manifold that allows for direct pressure measurement and control, the sample was lowered into the high field NMR. From there a spectrum was taken at the desired pressure. Once the spectra are taken, the calibration curve can be constructed. Each methane signal was normalized by dividing it by the constant signal from the D_2O inside the capillary. Then the measured pressure was used to calculate the density of the vapor phase in REFPROP. This density was then normalized by the number of protons in the calibrant gas to ultimately calculate the "Proton Density". Similar to Suiter et al.[12], this calibration curve was expected to be linear (Figure 36).

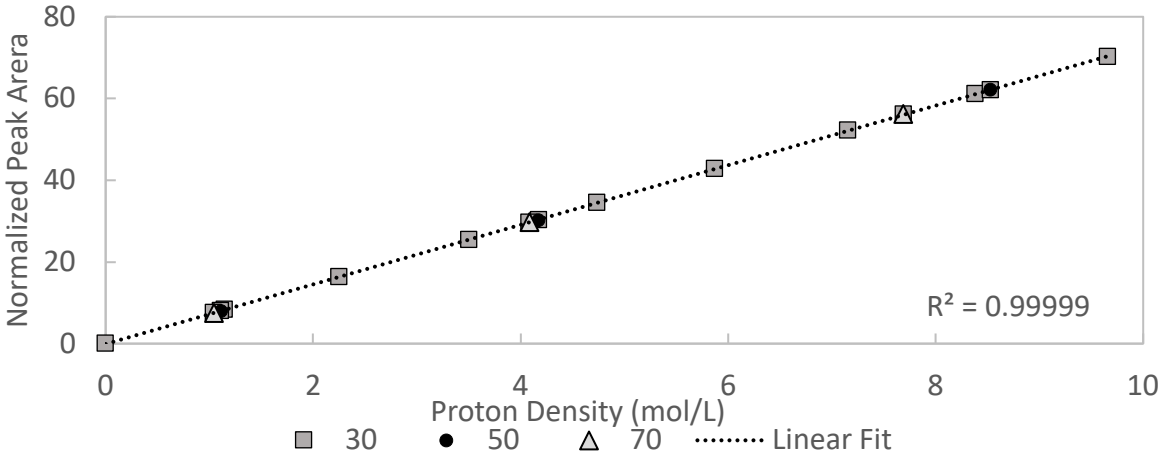

Figure 36: Calibration curve for vapor phase density with a D_2O filled capillary at 3 different temperatures and ranging pressures up to 5.51 MPa.

4.3. VLE MEASUREMENT RESULTS

The liquid component of the VLE measurement of methane and water were taken at 299.65 K and measured on the benchtop NMR instrument. The pressure range studied went up to 2.07 MPa (Table 1). The high field instrument's data collection is discussed but not reported due sample equilibrium not being achieved.

Table 1: Measured liquid components of the binary system methane + water at various pressures on the benchtop instrument at 299.65 K.

System	P (MPa)	$X_{liq,1}$ mole frac CH_4	$X_{liq,2}$ mole frac H_2O
(Methane + Water)	1.20E-01	1.55E-05	9.99985E-01
	3.51E-01	6.60E-05	9.99934E-01
	6.91E-01	1.45E-04	9.99855E-01
	1.06E+00	2.49E-04	9.99751E-01
	1.39E+00	3.02E-04	9.99698E-01
	1.74E+00	3.54E-04	9.99646E-01
	2.07E+00	4.43E-04	9.99557E-01

4.4. DISCUSSION ON VLE RESULT

The experimental data collected in this study was liquid phase at low pressures. The data collected exhibited the expected trend that the concentration of methane will increase with pressure (Figure 37). This trend was initially predicted with REFPROP calculations (Section 3.6).

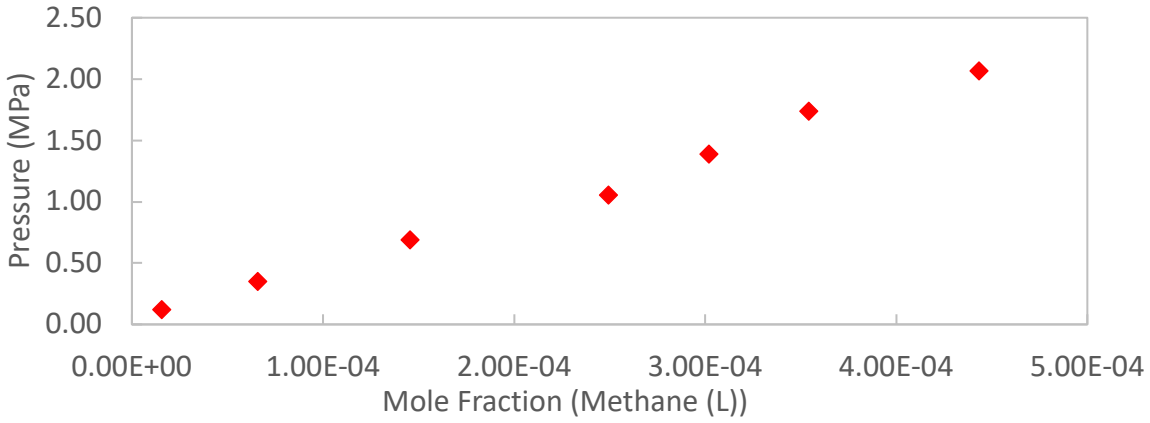

Figure 37: The measured concentrations of methane dissolved in water at various pressures.

The experimental difficulty of this system, and the rigors that had to be addressed prior to data collection, should be discussed. The initial measurement technique explored for measuring both liquid and vapor phase composition in a single spectrum were halted when the preliminary studies revealed the overlapping signals. This forced us to separate the measurement into two experiments: liquid and vapor. The separation of these two measurements does not affect the equilibrium results. As discussed in Section 1.3, the defining parameters in a VLE experiment are the thermodynamic conditions that the sample is experiencing. This in conjunction with the NMR measurements which produce relative compositions, means that gravimetric sample preparation is not necessary. This is one of the largest advantages of this experimental method.

The resulting compositions measured on the benchtop instrument for the liquid phase VLE data (Table 1) brings up the validity of each instruments' measurements. The benchtop dataset was taken with sample composition of 100% H_2O while the high field instrument's samples were made from 90% D_2O + 10% H_2O. The reasons for this composition change between data sets was related to the high-field instrument's tolerance for highly protonated fluids and its shimming and signal locking protocols. Due to its high sensitivity, a spectrum with 100% H_2O produces a water signal that overlaps the methane. Additionally, a lot of instrument time would be spent manually shimming to produce a sharp signal. To take advantage of automated shimming, some portion of the sample must contain a deuterated fluid e.g., D_2O. With all of these factors, the most reasonable solution was to change the composition of the sample and study the solubility differences.

The compositional differences in this liquid phase sample introduce potential solubility differences between methane and H_2O/D_2O. With these differences documented[25,26], our focus went to measure the difference ourselves. Here we ran several different compositions of H_2O and D_2O ranging from 100% to 0% increments of 25%. The results from this experiment are shown in

Figure 38. The resulting conclusion was that higher the percentage of water the less methane would be able to dissolve into it. This is similar solubility difference as the reported in literature sources[25,26].

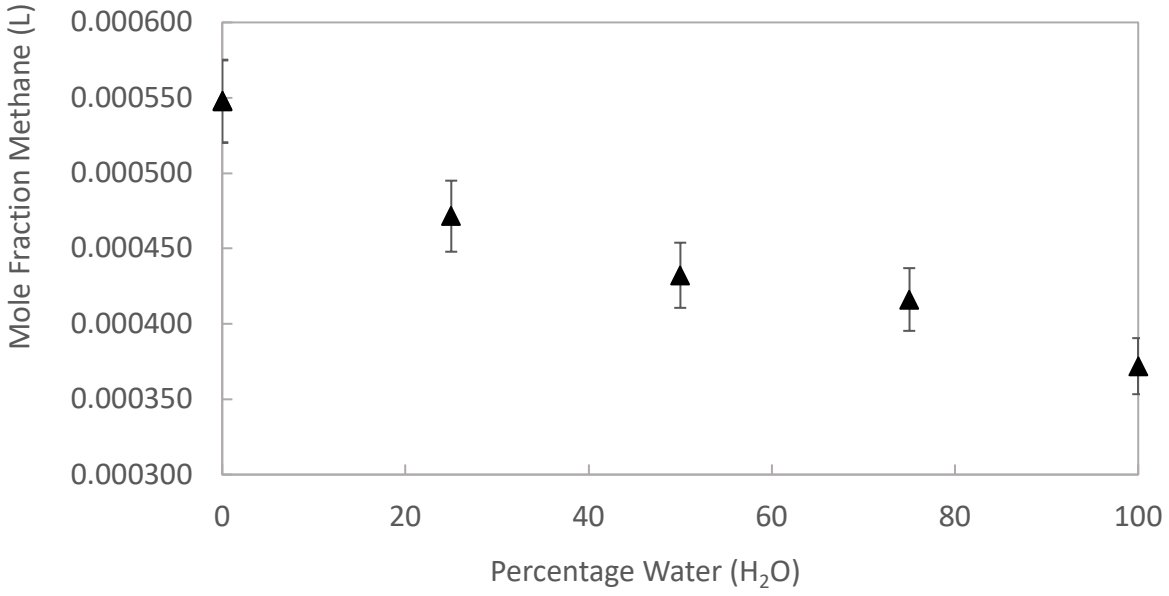

Figure 38: The average mole fraction measured of a sample of $\%H_2O$ and $\%D_2O$ at 1.72 MPa and 26.5°C. These were averaged over six data collections from the same sample.

This difference in solubilities is significant. This solubility discrepancy can be extrapolated and accounted for after data collection when the high-field instrument data is taken. This comparison was done with the large instrument at low pressures, possibly requiring this to be done at multiple pressures to accurately see the deviation between the two concentrations.

4.5. COMPARISON TO REFRPOP, HENRY'S LAW AND LITERATURE

The liquid phase VLE data (Table 1) was considerably different than in the equation of state (REFPROP) prediction. This discrepancy can be seen when plotting the collected data and the REFPROP prediction (Figure 39)

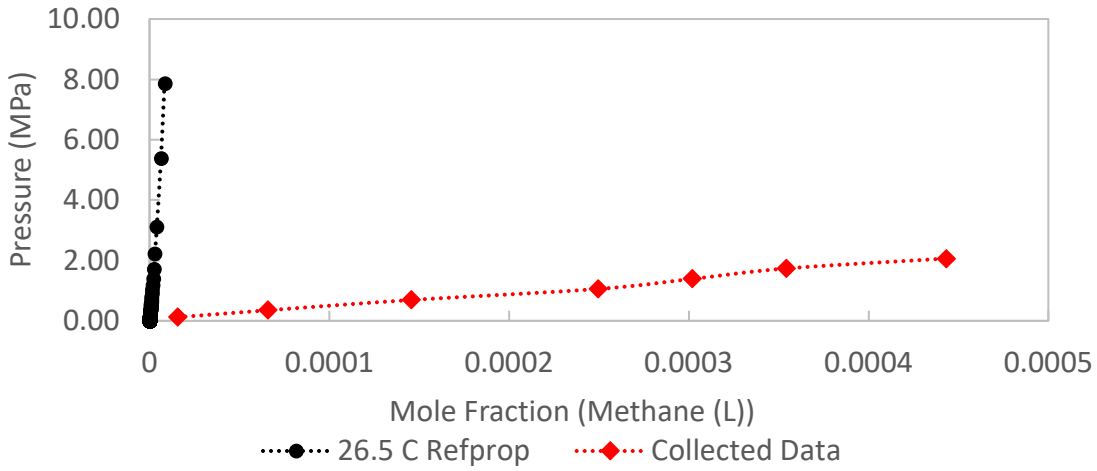

Figure 39: The predicted equilibrium values of dissolved methane (L) in water at 26.5°C compared to the measured values of dissolved methane in water using the benchtop instrument.

A quite different comparison happens when looking at methane solubility studies from the literature. The data collected in this work agree closely with those solubility studies (Figure 40). Comparing the literature data to both REFPROP and this works data reveals significant shortcomings with this software's predictions (Figure 40).

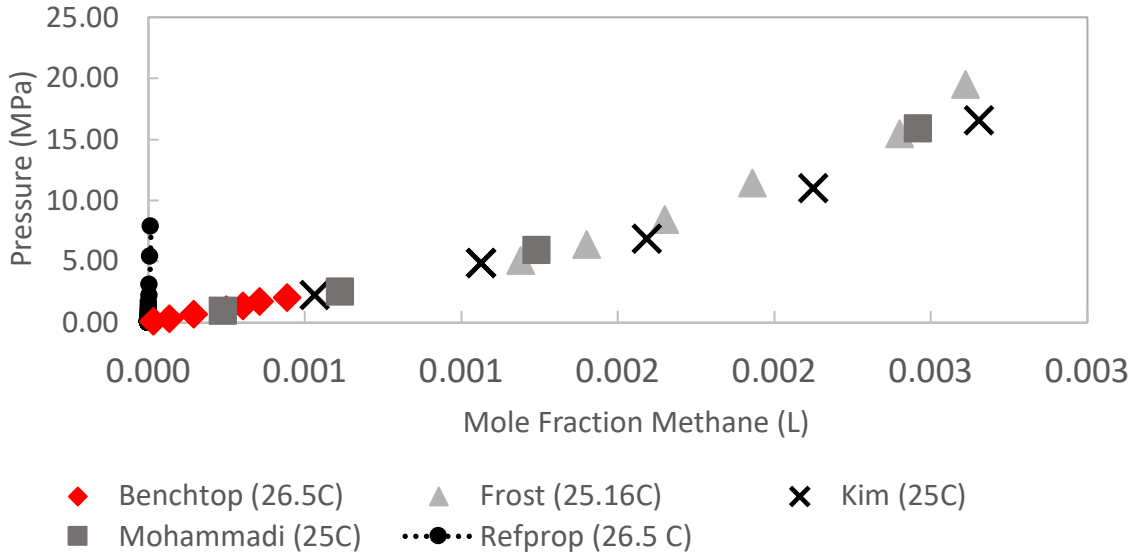

Figure 40: Collected liquid phase data with both literature sources and REFPROP's prediction. Notice that REFPROP is not close to any of the collected data. Frost et al.[8], Mohammadi et al.[11] and Kim et al.[9]

After preliminary results showed this discrepancy between REFPROP and our findings, we consulted with one of the developers of REFPROP[27]. They mentioned that the REFPROP model was developed without liquid-phase data. In order to check the predictions of REFPROP and our measured data, Henry's Law was used (See section 1.3). Appropriate constants and parameters were utilized and compared to the current work and REFPROP (Figure 41)

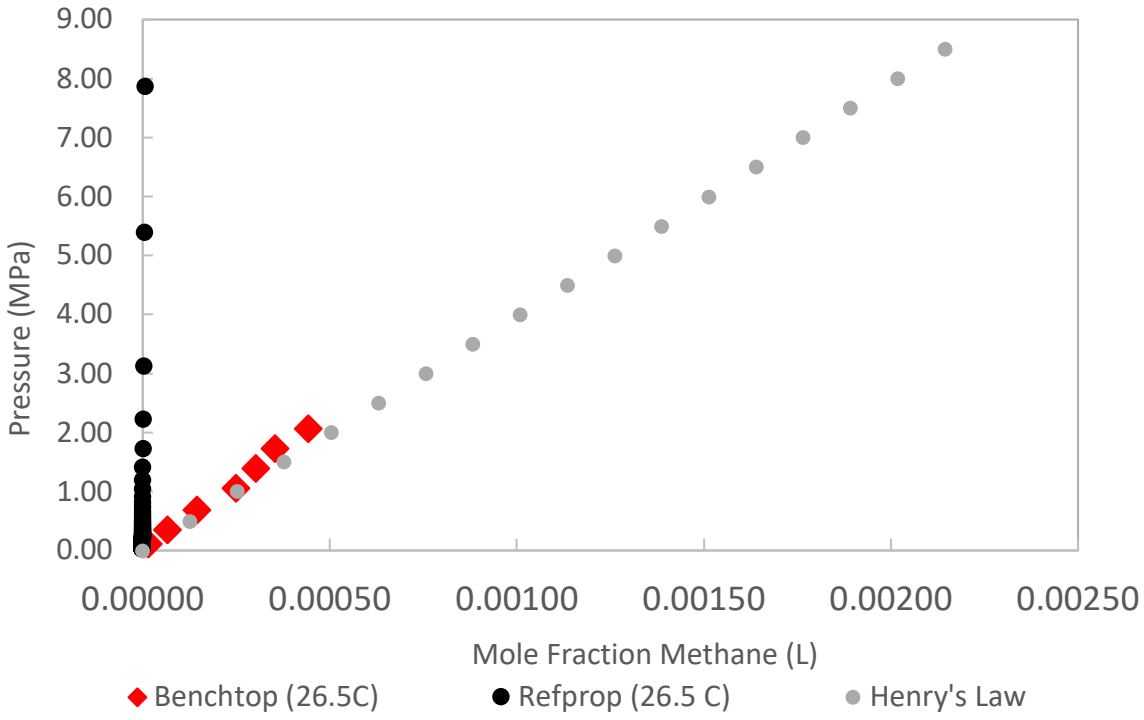

Figure 41: The data collected compared to both REFPROP and Henry's law.

This simple comparison demonstrates that the REFPROP equation of state is not consistent with relevant liquid phase data.

5. CONCLUSIONS

This study investigated the vapor liquid equilibrium of methane and water at various pressures. The method used in this data collection has improvements over the conventional method of a gas chromatography. The advantages are the direct measurements with no sample separation, no calibration, instrument sensitivity, measurement repeatability, and no reliance on gravimetric sample preparation. This work ultimately focused on both the development of experimental methods for both liquid and vapor phases and low-pressure liquid phase measurements. The ultimate goal was to measure high quality data of liquid equilibrium, and to provide it to the developers of REFPROP. This high-quality data would then be used to improve the accuracy of the predictive equation of state software. This improvement to the accuracy of the REFPROP models would help the natural gas compressor operators and designers achieve higher efficiencies and come closer to the operational limits.

Key conclusions from this work are as follows:

- The vapor liquid equilibrium for a system of methane and water is difficult to measure. There were several unexpected challenges that arose throughout. First, when testing the capabilities of the benchtop instrument, water vapor was not able to be detected. Second, when trying to measure all signals in the system in one spectrum, the capillary and water signals were found to overlap. Third, the equilibration time on the benchtop was shorter than on the high field instrument. Finally, the pressure was not able to be measured directly due to the possibility of water vapor condensing inside the transfer line. With all of these

challenges, solutions were developed and implemented to carryout partial VLE measurements for a wide range of pressures. This work is a key steppingstone to complete VLE measurements on important systems similar to methane and water.

- The resulting predictions from REFPROP extremely under predict the measured methane content dissolved in water. This large discrepancy between REFPROP, the current work, literature data, and Henry's Law reveal the necessity of high quality VLE data for this system. Ultimately, this difference provides cause to suspect that additional predictions for this system could be incorrect.
- The effect that this has on the end user (i.e., natural gas industry) is that a different set of design conditions could be calculated due to the better predictions from the EOS software. These changes in calculated design conditions could result in a reduction of transportation costs.

5.1. FUTURE WORK

Moving forward, there are a few details that should be addressed prior to moving to new systems with this measurement technique. First, additional measurements are needed to extend the scope of the liquid phase measurement by varying the temperature within the high field instrument. Next area of study should be the completion of this systems vapor phase measurement. This will require the use of the capillary and the vapor phase density calibration (as described in Section 4.2.1.) to determine the pressure inside the sample at the time of data collection. Following this data collection, additional development on pressure measurement techniques would greatly improve the overall process of liquid phase measurement. Finally, carry this methodology over to several other systems that include CO_2 and heavier hydrocarbons (e.g., C7 +) to help improve these EOS solutions.

REFERENCES:

[1] "U.S. Energy Facts Explained - Consumption and Production - U.S. Energy Information Administration (EIA)." *U.S. Energy Facts Explained*, U.S. Energy Information Administration (EIA), www.eia.gov/energyexplained/us-energy-facts. Accessed 2 Mar. 2021.

[2] "About Natural Gas." *Southwest Gas*, Southwest Gas, www.swgas.com/en/learn-about-energy. Accessed 3 Mar. 2021.

[3] "EIA - Natural Gas Pipeline Network - Transporting Natural Gas in the United States." *About US Naturalizations*, The US Energy Information Association, www.eia.gov/naturalgas/archive/analysis_publications/ngpipeline/index.html. Accessed 2 Mar. 2021.

[4] Calma, Justine. "Texas' Natural Gas Production Just Froze Under Pressure." *The Verge*, 17 Feb. 2021, www.theverge.com/2021/2/17/22287130/texas-natural-gas-production-power-outages-frozen.

[5] Adewumi, Michael. "Introduction | PNG 520: Phase Behavior of Natural Gas and Condensate Fluids." *Penn State*, www.e-education.psu.edu/png520/m12_p2.html. Accessed 1 Mar. 2021.

[6] Kunz, O., and W. Wagner. "The GERG-2008 Wide-Range Equation of State for Natural Gases and Other Mixtures: An Expansion of GERG-2004." *Journal of Chemical & Engineering Data*, vol. 57, no. 11, 2012, pp. 3032–91. *Crossref*, doi:10.1021/je300655b.

[7] McLinden, Mark O., and Markus Richter. "Application of a Two-Sinker Densimeter for Phase-Equilibrium Measurements: A New Technique for the Detection of Dew Points and

Measurements on the (Methane + Propane) System." *The Journal of Chemical Thermodynamics*, vol. 99, 2016, pp. 105–15. *Crossref*, doi:10.1016/j.jct.2016.03.035.

[8] Frost, Michael, et al. "Vapor–Liquid Equilibrium of Methane with Water and Methanol. Measurements and Modeling." *Journal of Chemical & Engineering Data*, vol. 59, no. 4, 2013, pp. 961–67. *Crossref*, doi:10.1021/je400684k.

[9] Kim, Y. S., et al. "Liquid Water−Hydrate Equilibrium Measurements and Unified Predictions of Hydrate-Containing Phase Equilibria for Methane, Ethane, Propane, and Their Mixtures." *Industrial & Engineering Chemistry Research*, vol. 42, no. 11, 2003, pp. 2409–14. *Crossref*, doi:10.1021/ie0209374.

[10] Simons, Sarah B., "Dew Point Benchmarking Measurements" Southwest Research Institute. Accessed 5 Mar. 2021.

[11] Mohammadi, Amir H., et al. "Gas Solubility: A Key to Estimating the Water Content of Natural Gases." *Industrial & Engineering Chemistry Research*, vol. 45, no. 13, 2006, pp. 4825–29. *Crossref*, doi:10.1021/ie051337i.

[12] Suiter, Christopher L., et al. "Nuclear Magnetic Resonance (NMR) Spectroscopy for the In Situ Measurement of Vapor–Liquid Equilibria." *Journal of Chemical & Engineering Data*, vol. 65, no. 7, 2020, pp. 3318–33. *Crossref*, doi:10.1021/acs.jced.0c00113.

[13] "Henry's Law" www.chem.libretexts.org/@go/page/1599. Accessed 10 Mar. 2021.

[14] "Raoult's Law" www.chem.libretexts.org/@go/page/1598. Accessed 10 Mar. 2021.

[15] Claridge, Timothy. *High-Resolution NMR Techniques in Organic Chemistry*. 3rd ed., Elsevier Science, 2016.

[16] “U28-E05. Bruker Avance 600 MHz NMR Spectrometer + HR-MAS Probe | Nanbiosis.” *NonBiosis*, www.nanbiosis.es/u28-e05-bruker-avance-600-mhz-nmr-spectrometer-hr-mas-probe. Accessed 4 Mar. 2021.

[17] “Magritek | Spinsolve 60 MHz.” *Magritek*, magritek.com/products/spinsolve/spinsolve-60. Accessed 3 Mar. 2021.

[18]“Nuclear Magnetic Resonance Laboratory.” *NIST*, www.nist.gov/mml/acmd/fluid-characterization-group/nuclear-magnetic-resonance-laboratory. Accessed 5 Mar. 2021.

[19]“Daedalus Innovations | High Pressure NMR.” *Daedalus Innovations*, daedalusinnovations.com/high-pressure-nmr. Accessed 1 Mar. 2021.

[20] Farrar, Thomas C., et al. “Oxygen-17-Induced Proton Relaxation Rates for Alcohols and Alcohol Solutions.” *Journal of the Brazilian Chemical Society*, vol. 10, no. 4, 1999. *Crossref*, doi:10.1590/s0103-50531999000400012.

[21]“Temperature Calibration - Wiki.” *Temperature Calibration*, www.nmr2.buffalo.edu/nesg.wiki/Temperature_calibration. Accessed 4 Mar. 2021.

[22]“Cernox®.” *Default*, www.lakeshore.com/products/categories/overview/temperature-products/cryogenic-temperature-sensors/cernox. Accessed 6 Mar. 2021.

[23]“NMR Consumables > Gas Tight > High Pressure/Vacuum | Wilmad-LabGlass.” *Pressure/Vacuum 5 Mm OD NMR Tubes*, www.wilmad-labglass.com/ProductList.aspx?t=449. Accessed 7 Mar. 2021.

[24]“VLE Diagram · Issue #79 · Usnistgov/REFPROP-Issues.” *GitHub*, github.com/usnistgov/REFPROP-issues/issues/79. Accessed 8 Mar. 2021.

[25] Wilhelm, Emmerich., et al. “Low-Pressure Solubility of Gases in Liquid Water.” *Chemical Reviews*, vol. 77, no. 2, 1977, pp. 219–62. *Crossref*, doi:10.1021/cr60306a003.

[26] Cosgrove, Bruce A., and John Walkley. “Solubilities of Gases in H2O and 2H2O.” *Journal of Chromatography A*, vol. 216, 1981, pp. 161–67. *Crossref*, doi:10.1016/s0021-9673(00)82344-4.

[27] E. Lemmon, personal communication, January 11, 2021.